AD NUMBER

AD-384 956

CLASSIFICATION CHANGES

TO   **UNCLASSIFIED**

FROM   **CONFIDENTIAL**

AUTHORITY

USARRADCOM Notice, dtd August 31, 1982.

19990301074

UNCLASSIFIED

AD NUMBER

AD-384 956

NEW LIMITATION CHANGE

TO

DISTRIBUTION STATEMENT - A

Approved for Public Release; Distribution Unlimited.

LIMITATION CODE - 1

FROM

DISTRIBUTION STATEMENT - NONE

No Prior DoD Distribution Security Control Statement.

AUTHORITY

USAARDCOM Notice, dtd August 31, 1982.

THIS PAGE IS UNCLASSIFIED

REPRODUCTION QUALITY NOTICE

This document is the best quality available. The copy furnished to DTIC contained pages that may have the following quality problems:

- Pages smaller or larger than normal.

- Pages with background color or light colored printing.

- Pages with small type or poor printing; and or

- Pages with continuous tone material or color photographs.

Due to various output media available these conditions may or may not cause poor legibility in the microfiche or hardcopy output you receive.

☐ If this block is checked, the copy furnished to DTIC contained pages with color printing, that when reproduced in Black and White, may change detail of the original copy.

AD

L3300-1-68-

TECHNICAL REPORT R-1860

A SOURCE OF SMALL ARM MUZZLE NOISE (U)

by

Leonard W. Skochko
Harry A. Greveris

AMCMS Code 5542.12.46806.01

DA Project No. MI-5-16495-06-F6-NH

In addition to security requirements which apply to this document and which must be met, this document is subject to special export controls and each transmittal to foreign governments or foreign nationals may be made only with prior approval of Commanding Officer Frankford Arsenal, Philadelphia, Pa. 19137 — ATTN: SMUFA

AUGUST 1967

UNITED STATES ARMY
FRANKFORD ARSENAL
PHILADELPHIA, PA.

SECURITY

MARKING

The classified or limited status of this report applies to each page, unless otherwise marked.

Separate page printouts MUST be marked accordingly.

DISPOSITION INSTRUCTIONS

WARNING NOTICES

TECHNICAL REPORT R-1860

A SOURCE OF SMALL ARM MUZZLE NOISE   (U)

by

Leonard W. Skochko
Harry A. Greveris.

AMGMS Code 5542.12.46801.01

DA Project No.-M1-5-16495-06-F6-NH

In addition to security requirements which apply to this document and which must be met, this document is subject to special export controls and each transmittal to foreign governments or foreign nationals may be made only with prior approval of Commanding Officer, Frankford Arsenal, Philadelphia, Pa.   19137 - ATTN: SMUFA-J8100.

Ammunition Development and Engineering Laboratories
FRANKFORD ARSENAL
Philadelphia, Pa.   19137

AUG 1967

DDC CONTROL
NO. 74513

(U)   ABSTRACT

        This report describes and analyzes the pressure wave generated
in front of small caliber subsonic projectiles traveling in gun barrels.

        Equations are developed to predict the precursor wave sound
signature in the far field.

        Calculations and measured sound data are presented for several
representative, conventional and unconventional, small arm weapons.

TABLE OF CONTENTS

TABLE OF ILLUSTRATIONS

LIST OF TABLES

LIST OF SYMBOLS

V_p = projectile velocity

P = static pressure

t = time

x = travel

C_s = precursor shock propagating velocity

u = flow velocity

a = sonic velocity

a_o = ambient air sonic velocity, 1130 fps

γ = air specific heat ratio, 1.4

V = propagating velocity

P_o = ambient air pressure, 14.7 psi

X = pressure pulse travel coordinate

T = pressure pulse time coordinate

$\left(\dfrac{dV_p}{dt}\right)$ = projectile acceleration

M_p = projectile Mach No. (V_p/a_o)

ΔS = air entropy change across shock

P_s = absolute pressure following shock

P_r = absolute pressure preceding shock

$\left(\dfrac{du}{dt}\right)$ = flow acceleration

A_p = projectile cross-section area

A_t = barrel or tube cross-section area

1 = projectile nose length, projectile length

$\left(\dfrac{dV_p}{dt}\right)_1$ = peak projectile acceleration

M_1 = projectile Mach No. at peak acceleration

x_1 = projectile travel at peak acceleration

K_1 = empirical constant, .79

K_2 = empirical constant, .97

K_3 = empirical constant, .78

v_o = propellant chamber volume

v_c = propellant volume

k = propellant gas ratio of specific heats (~ 1.2)

P_1 = peak propellant gas pressure

m = projectile mass

X_o = precursor shock formation distance

$\left(\dfrac{d_m^2}{dt^2}\right)$ = mass flow rate change per time

r = distance to sound source

V_r = rarefaction head propagating velocity

t_r = time for rarefaction to reach projectile

l_o = precursor pressure column length

t_e = time for rarefaction to return at muzzle

$\dot{m}_m$ = precursor air mass flow at muzzle

t_p = time between precursor shock and projectile exits at muzzle

P_m = maximum precursor sound pressure

f = fundamental jet frequency, effective sound pulse frequency

d = jet and gun barrel diameter

P_n = precursor rarefaction negative sound pressure

L_m = peak precursor sound pressure level (SPL)

θ = azimuth angle from line of fire at gun

$\left(\dfrac{d^2 v}{dt^2}\right)$ = volumetric displacement rate change per time

ρ_o = ambient air density (at . 70° F), . 30 grains/inches^3

T_a = sound pulse time duration (short projectile)

T_1 = sound pulse time duration (long projectile)

$\left(\dfrac{dv}{dt}\right)$ = volumetric displacement rate

INTRODUCTION

(U)   The general noise problem of the so-called "silent" or "low sig-nature" small arms weapons may be classified into four categories.[1]

1. Mechanical weapon noise:

    a.   Gun component motion, impact, vibration, etc.

    b.   Aerodynamic noise: air pocket compression, reverbera-tions, amplification, gas leakage, etc.

2. Weapon muzzle noise:

    a.   Pressures ahead of projectile: precursor wave phenomenon, blow-by, etc.

    b.   Projectile muzzle exit: physical air volume displacement.

    c.   Projectile base pressure discharge: propellant gas, vacuum, etc.

3. Projectile flight noise:[2]

    a.   Supersonic projectile: ballistic crack.

    b.   Subsonic projectile: air turbulence, "Karman vortex street", pressure field excitation, etc.

4. Target impact noise:

    a.   Hard objects and surfaces.

    b.   Soft objects and surfaces.

(U)   The fifth possible category, the objections of the human target to being fired upon, naturally was omitted.

---

[1]See References

(U)   The contents of this report are intended to shed a little light on one of the still not fully defined gaps in design and evaluation of low signature small arms weapons. Specifically, to be described are the phenomenon occurring ahead of the subsonic projectile traveling in a gun barrel and the sound pressures resulting from this phenomenon in the fair field.

(U)   A projectile traveling in a gun barrel compresses the air immediately ahead of it.   The precursor pressure wave thus generated, even with subsonic projectiles, is substantial and causes concern when the weapon is being designed for low sound output. However, to be able to design for or limit the noise due to this precursor pressure wave, it is first necessary to describe both physically and analytically the generation of such a wave and, lastly, to relate the parameters of this precursor pressure wave to the noise in the far field.

(U)   For predicting the parameters of the precursor pressure wave in the gun barrel, it was found necessary to use the method of characteristics along with a few simplifying assumptions. Although the general approach to be described is not uncommon and is well substantiated with experimental data from shock tubes, the data directly pertinent to this report is scarce.   This is especially true of several unique problems considered herein.

(U)   Correlation of the precursor pressure wave in the gun barrel with the corresponding far field sound effect is somewhat involved. Very little analytical and experimental work directly pertinent to the subject has been published. Further, linearized acoustical techniques almost completely fail when applied directly to high temperature, pressure and velocity gas flows encountered in guns. Since a sound generating tube, to a certain extent, behaves like a simple acoustical point source, the analogy was extended to the discharge of precursor wave from the gun barrel. This technique seems to yield a reasonable prediction of the precursor wave sound pressure history in the far field.

(S)   For treating the more complex weapon systems with barrel discontinuities, it was first necessary to consider such problems as a projectile traveling in an oversized tube and a projectile entering a tunnel in a wall. Combination of the effects in these simple problems allows an estimate of what can be expected in such systems as the XM202, a low signature, pressure sustaining cartridge.

2

(U)   Generally, the complete projectile acceleration history is neces-
sary to predict the precursor pressure wave parameters in the gun bar-
rel. However, often the weapon of interest may have only the peak gun
pressure and projectile muzzle velocity specified. These, in addition
to propellant properties and physical weapon description, were found
sufficient to obtain a rough estimate of precursor shock formation in
the given weapon. Thus a preliminary weapon evaluation is possible
without complete internal ballistic data.

ANALYSIS

(U)   To determine analytically the complete precursor pressure
wave ahead of the projectile, it was found expedient to make the follow-
ing preliminary assumptions:

        1.   The precursor pressure wave is a plane wave, so that all
air flow in the gun barrel is one dimensional. This assumption is pos-
sible when the precursor wave length is much larger than the projectile
nose length.

        2.   Heat transfer to the barrel and projectile is insignificant,
since the temperature gradient is low and exists only for a short time.

        3.   Isentropic relations hold throughout except across a strong
shock.

        4.   Linearized acoustical equations are applicable to small
pressure increments within the precursor pressure wave.

(U)   The above assumptions, along with the inherent inaccuracies of
the method of characteristics, simplify the problem substantially and
yet yield relatively small errors in computation.

A.   Piston in Smooth Tube[3, 4, 5, 6]

(U)   Consider now a piston in a smooth tube starting from rest and
accelerating into air that has no initial flow velocity with respect to
the tube (see figure 1).

3
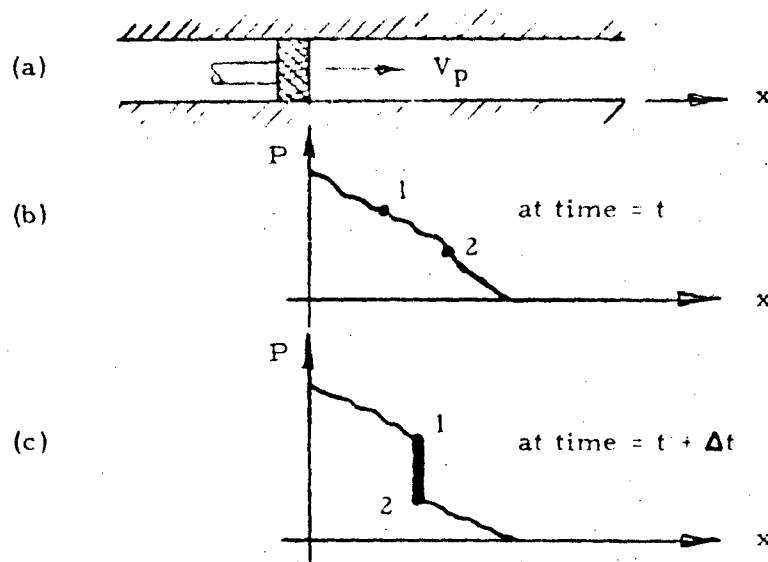
Figure 1. (U)   Precursor Wave Formation Ahead of an
                Accelerating Piston in a Tube

(U)   As the piston travels down the tube, it compresses the air im-
mediately ahead of it.   This local disturbance creates a transient pres-
sure wave which propagates down the tube.   Each given pressure point
within the wave (pts. 1 and 2, figure 1b and 1c) propagates at the velocity
equivalent to the sum of local sonic and flow velocities.   These sonic and
flow velocities as well as pressure and temperature are higher nearer
the piston due to piston acceleration.   Because of the gradient thus es-
tablished, pressure point 1 overtakes pressure point 2.   At any given
time the instantaneous pressure at any given point in the wave beyond
the piston will be some sort of a sum of various pressures initiated
earlier and which have arrived at the point and time in question.   At
the first mergence of two different pressures, a shock is formed.   The
magnitude of this shock is generally transient and depends on reinforce-
ment by increasingly higher pressures generated by the moving piston.

(U)   For computational purposes let us now approximate the precur-
sor pressure wave profile of figure 1a by a pressure gradient consisting
of a series of small pressure pulses shown in figure 2b.   The piston may
be looked upon as moving in a step manner to produce the given series
of compression waves which propagate down the tube ahead of the piston.

4
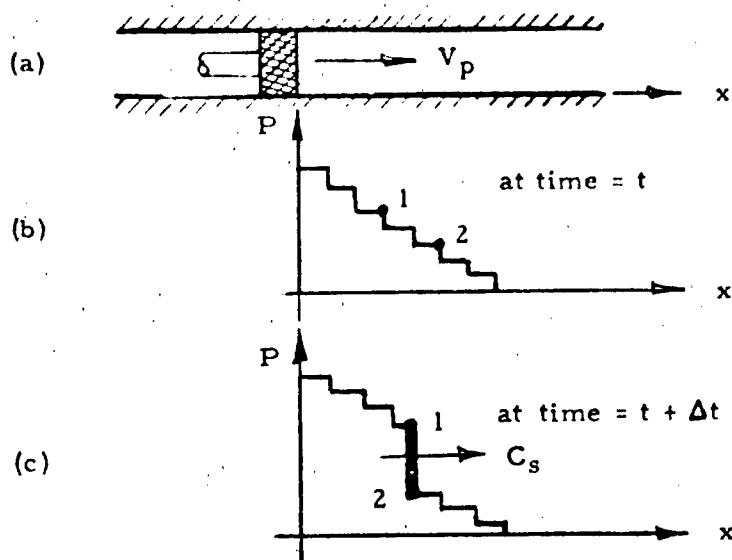
Figure 2. (U) Precursor Wave Represented by Increments
for Computation

(U)   Each of these pressure pulses travels with the local speed of
sound relative to the air through which it passes. Thus, the given
pressure pulse velocity,

$$v = u + a \qquad (1)$$

where u is the local air flow velocity and a is the local air sonic ve-
locity. In a sound wave the local sonic velocity is

$$a = a_o + \frac{\gamma - 1}{2} u \qquad (2)$$

where a_o is the air sonic velocity prior to arrival of the sound wave
and γ is the air ratio of specific heats.

(U)   Combining the two above equations, the given pressure pulse is
found to propagate at velocity

$$v = a_o + \frac{\gamma + 1}{2} u \qquad (3)$$

5

which is seen to depend only on the local air flow velocity. At any given time the air particles adjacent to the piston face travel at the same velocity as the piston. Thus, by applying Equations 2 and 3 to the air adjacent to the piston face, both the sonic velocity and velocity of propagation of the pressure pulses generated by the piston become known. Further, since an isentropic process can be assumed for air compression by the piston, the absolute pressure of the given pressure pulse generated by the piston face is

$$P = P_0 \left(\frac{a}{a_0} \right)^{2\gamma / \gamma - 1} \tag{4a}$$

or

$$P = P_0 \left(\frac{a_0 + \frac{\gamma - 1}{2} u}{a_0} \right)^{2\gamma / \gamma - 1} \tag{4b}$$

where P_0 is the atmospheric air pressure prior to compression by the piston and u is V_p, the instantaneous projectile velocity.

(U)   The travels of piston and given piston generated pressure pulse with time are represented graphically in figure 3. Here the pulse travel is shown as a straight line, which indicates that once a given pressure pulse is generated, it propagates at a constant velocity until overtaken by a faster propagating pressure pulse. The propagating velocity (straight line slope) of the given pulse, of course, depends on initiating projectile velocity (Eq 3). The faster a piston travels, the higher the face pressure it generates and the faster this pressure magnitude (or pressure pulse) propagates forward. Location of a given pressure pulse at time, T, is

$$X = (T - t) \left(a_0 + \frac{\gamma + 1}{2} V_p \right) + x \tag{5}$$

where t, V_p, and x are respectively the instantaneous time, piston velocity and piston location when the given pulse originated.

6
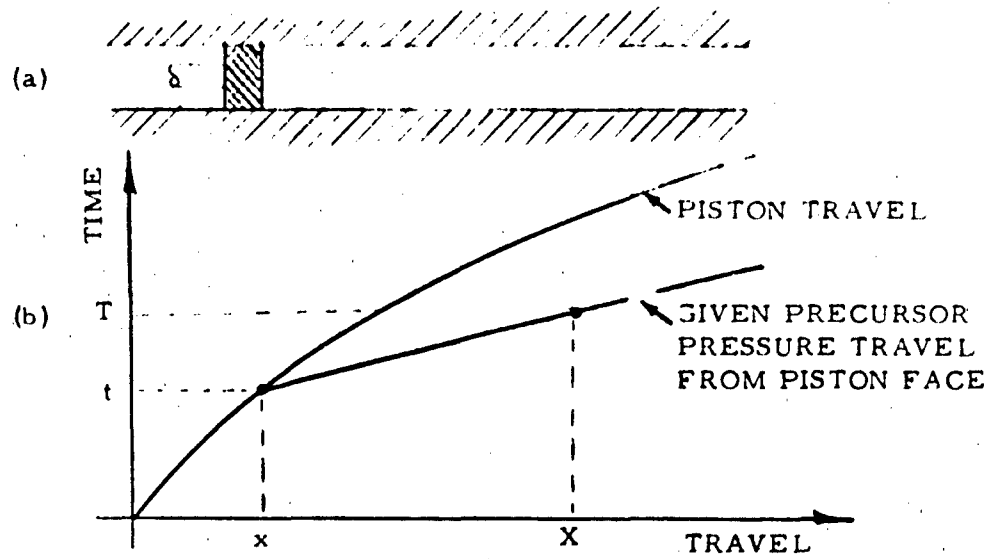
Figure 3. (U) Piston and Generated Pressure Propagation
Along the Tube

(U)   When any two pressure pulses merge, a discontinuity (shock) is
formed. To find the intersection point of two consecutive pulses genera-
ted by an accelerating piston, it is necessary to combine Equation 5
with the one derived from it by partially differentiating it with respect
to time. The result is a parametric set of equations with time as a
parameter.

$$X = \left(\frac{2}{\gamma + 1}\right)\left[\frac{\left(a_0 + \frac{\gamma - 1}{2} V_P\right)\left(a_0 + \frac{\gamma + 1}{2} V_P\right)}{\left(\frac{d V_P}{dt}\right)}\right] + x \qquad (6a)$$

and

$$T = \left(\frac{2}{\gamma + 1}\right)\left[\frac{\left(a_0 + \frac{\gamma - 1}{2} V_P\right)}{\left(\frac{d V_P}{dt}\right)}\right] + t \qquad (6b)$$

where X and T represent the location and time of discontinuity for-
mation due to given piston velocity and acceleration.

7

(U) By simplifying and factoring out a_0, Equations 6 becomes

$$X = \left(\frac{2a_0^2}{\gamma + 1}\right)\left[\frac{1 + \gamma M_p + \frac{\gamma^2 - 1}{2} M_p}{\left(\frac{d V_p}{dt}\right)}\right]^2 + x \tag{7a}$$

and

$$T = \left(\frac{2a_0}{\gamma + 1}\right)\left[\frac{1 + \frac{\gamma - 1}{2} M_p}{\left(\frac{d V_p}{dt}\right)}\right] + t \tag{7b}$$

where M_p is instantaneous piston Mach No., (V_p/a_0).

(U) Further, since for subsonic projectiles $\frac{\gamma^2 - 1}{4} M_p \ll 1 + \gamma M_p$ and $\frac{\gamma - 1}{2} M_p \ll 1$, Equations 7 simplify to

$$X \approx \left(\frac{2a_0^2}{\gamma + 1}\right)\left[\frac{1 + \gamma M_p}{\left(\frac{d V_p}{dt}\right)}\right] + x \tag{8a}$$

and

$$T \approx \left(\frac{2a_0}{\gamma + 1}\right)\left[\frac{1}{\left(\frac{d V_p}{dt}\right)}\right] + t \tag{8b}$$

The location and time of the first mergence of precursor pressure gradient into a shock is defined by the least values of X and T of Equation 8.

(U) The propagation velocity of the formed precursor shock depends upon the shock pressure ratio and the air flow velocity just ahead of the shock (figure 2c). This dependence is expressed by

$$C_s = u_1 + a_1 \left[\frac{\gamma - 1}{2\gamma} + \frac{\gamma + 1}{2\gamma} \frac{P_2}{P_1}\right]^{1/2} \tag{9a}$$

8

or

$$C_s = u_1 + \left(a_0 + \frac{\gamma - 1}{2} u_1\right)\left[\frac{\gamma - 1}{2\gamma} + \frac{\gamma + 1}{2\gamma} \frac{P_2}{P_1}\right]^{1/2} \qquad (9b)$$

where C_s is shock propagating velocity, u_1 is the air flow velocity just ahead of the shock and P_1 and P_2 are absolute pressures, respectively just in front and just behind the shock.

(U)   The shock pressure ratio is defined in terms of the corresponding sonic velocities by

$$\frac{P_2}{P_1} = \left(\frac{a_2}{a_1}\right)^{2\gamma/\gamma - 1} e^{-\gamma \Delta s} \qquad (10)$$

where Δs is the entropy difference across the shock. Since the precursor shock pressure ratio for subsonic projectiles is relatively small it may be assumed that $e^{-\gamma \Delta s} \approx 1$ (see figure 4)
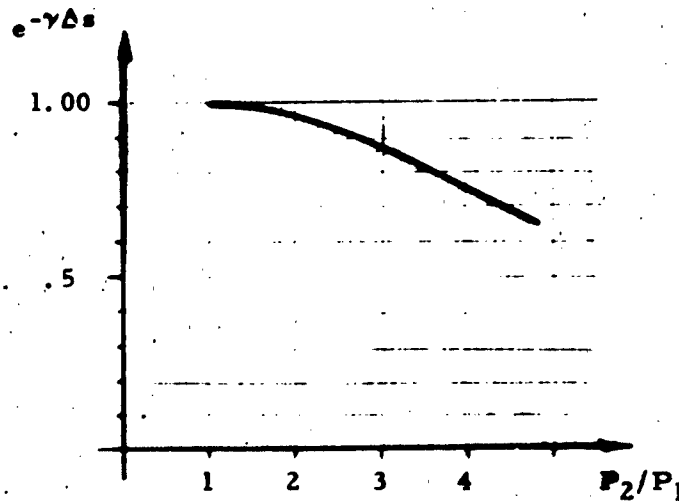
Figure 4. (U)   Entropy Term, $e^{-\gamma \Delta s}$ Magnitude in Equation 10

Therefore, Equation 10 may be simplified to

$$\frac{P_2}{P_1} = \left(\frac{a_2}{a_1}\right)^{2\gamma/\gamma-1} \tag{11}$$

which is an adiabatic relationship.

(U)   With Equation 11 the shock propagating velocity becomes

$$C_s = u_1 + \left(a_0 + \frac{\gamma-1}{2} u_1\right)\left[\frac{\gamma-1}{2\gamma} + \frac{\gamma+1}{2\gamma}\left(\frac{a_2}{a_1}\right)^{2\gamma/\gamma-1}\right]^{1/2} \tag{12a}$$

or

$$C_s = u_1 + \left(a_0 + \frac{\gamma-1}{2} u_1\right)\left[\frac{\gamma-1}{2\gamma} + \frac{\gamma+1}{2\gamma}\left(\frac{a_0 + \frac{\gamma-1}{2} u_2}{a_0 + \frac{\gamma-1}{2} u_1}\right)^{2\gamma/\gamma-1}\right]^{1/2} \tag{12b}$$

where the subscripts 1 and 2 refer to the conditions in front of and behind the shock front respectively.

(U)   Following is the method for finding the location and magnitude of the precursor shock wave at any time as it travels down the tube.

(U)   First the known position-time curve of the piston is drawn in the travel-time diagram (see figure 5). The smallest possible values of X and T (X_0 and T_0, corresponding to V_{p_0}, x_0 and t_0) are found from Equations 8. This is the point where the precursor shock first forms.

10
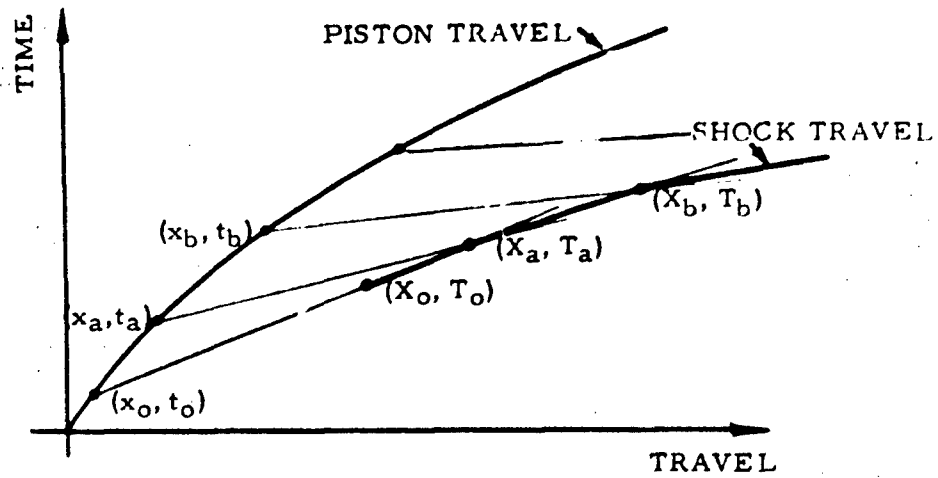
Figure 5. (U) Piston and Precursor Shock Travel-Time
History

The shock velocity from point X_0, T_0 is found from Equations 12 as

$$C_{s_0} = a_0 + \frac{\gamma + 1}{2} V_{P_0} \tag{13}$$

The absolute pressure immediately behind the first formed shock from Equation 4b is

$$P_{s_0} = P_0 \left(\frac{a_0 + \frac{\gamma - 1}{2} V_{P_0}}{a_0} \right)^{2\gamma/\gamma - 1} \tag{14}$$

The pressure difference across the shock at X_0, T_0, of course. is zero. At t_a (a short time after t_0) the pressure at the piston face is higher, corresponding to higher piston velocity. This pressure magnitude, propagating faster than that generated at (x_0, t), will overtake the latter at

11

$$X_a = X_0 + \left[\frac{(X_0 - x_a) - \left(a_0 + \frac{\gamma + 1}{2} V_{P_a}\right) T_0 - t_a}{\left(a_0 + \frac{\gamma + 1}{2} V_{P_a}\right) - C_{s_0}} \right] C_{s_0} \quad (15a)$$

and

$$T_a = \frac{X_a - X_0}{C_{s_0}} + T_0 \quad\quad (15b)$$

where in this case C_{s_0} is $a_0 + \frac{\gamma + 1}{2} V_{P_0}$

(U)   The absolute pressure of the shock traveling from (X_a, T_a) is

$$P_{s_a} = P_0 \left[\frac{a_0 + \frac{\gamma - 1}{2} V_{P_a}}{a_0} \right]^{2\gamma/\gamma - 1} \quad\quad (16)$$

the same as the pressure at (x_a, t_a).

(U)   The absolute pressure preceding this shock is

$$P_{r_a} = P_0 \left[\frac{a_0 + \frac{\gamma - 1}{2} V_{P_0}}{a_0} \right]^{2\gamma/\gamma - 1} \quad\quad (17)$$

the same as the pressure at (x_0, t_0).

(U)   The propagating velocity of the shock from (X_a, T_a) is, per Equations 12,

$$C_{s_a} = V_{P_0} + \left(a_0 + \frac{\gamma - 1}{2} V_{P_0}\right)\left[\frac{\gamma - 1}{2\gamma} + \frac{\gamma + 1}{2\gamma} \right.$$

$$\left. \left(\frac{a_0 + \frac{\gamma - 1}{2\gamma} V_{P_a}}{a_0 + \frac{\gamma - 1}{2\gamma} V_{P_0}} \right)^{2\gamma/\gamma - 1} \right]^{1/2} \quad\quad (18)$$

12

(U)   The pressure difference across the shock at (X_a, T_a) is

$$\Delta P_{s_a} = P_{s_a} - P_{r_a} \qquad (19)$$

(U)   Having obtained the pressure magnitude and its propagating velocity at (X_a, T_a), the next point (x_b, t_b) on the piston curve is chosen. To determine values at (X_b, T_b), the process described above is repeated over again. Thus are found the piston face and the precursor shock pressures at any location in the tube.

B.   Projectile in an Oversized Tube

(U)   The air flow and the wave action ahead of a projectile traveling in a gun barrel of same diameter is one-dimensional and in all respects similar to that of the above piston and tube. This condition cannot be assumed for a projectile traveling in a tube or barrel of larger diameter than the projectile. Here the air displaced by the projectile not only flows in the forward direction, but also rearward around the projectile. Although this problem is very complex, for our purposes it may be solved in the following manner.

(U)   Consider a nonaccelerating projectile traveling in an over-sized, long tube. With no wave reflections occurring from tube ends, the flow processes near the projectile may be assumed steady. Next, consider a stationary volume in the vicinity of projectile nose, bound by tube, projectile and broken lines shown in figure 6. If these boundaries are so located that the average air flow velocity across rearward boundary is the same as across forward boundary, then the continuity equation may be applied to the air flow from the bound volume. For average air densities and flow velocities across the tube area, the continuity consideration yields

$$u \approx \left(\frac{A_p}{2A_t - A_p} \right) V_p \qquad (20)$$

where u is the air flow velocity, A_p and A_t are respectively projectile and tube cross section areas, and V_p is the projectile velocity (figure 6).

13
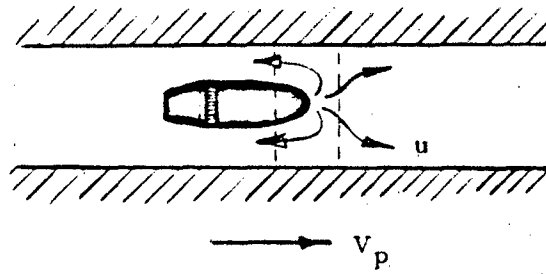
Figure 6. (U) Projectile Traveling in an Oversized Tube

(U)   By differentiation of Equation (21), the air flow accelera-
tion,

$$\left(\frac{du}{dt}\right) \approx \left(\frac{A_p}{2A_t - A_p}\right)\left(\frac{dV_p}{dt}\right) \tag{21}$$

where (dV_p/dt) is the projectile acceleration in a nonsteady flow case.

(U)   The average air pressure at the boundaries, from Equations
(2) and (4a), is

$$P \approx P_o\left[\frac{a_o + \frac{\gamma-1}{2}\left(\frac{A_p}{2A_t - A_p}\right)V_p}{a_o}\right]^{2\gamma/\gamma-1} \tag{22}$$

(U)   The propagating velocity of any given pressure magnitude is

$$V = a_o + \frac{\gamma+1}{2}\left(\frac{A_p}{2A_t - A_p}\right)V_p \tag{23}$$

14

(U)   To determine the complete precursor pressure wave of a projectile in an oversized tube, it is now only necessary to consider the forward boundary as a moving pressure source. Thus, the actual system is reduced to an "effective" simple piston-tube configuration, with the piston travel-time history that of the actual projectile. The piston face pressure, however, is determined from the projectile velocity modified by the factor $(A_p/2A_t - A_p)$. In all other respects the new system is solved by the method previously described.

C.   Projectile Entering a Tunnel

(U)   Similarly to a projectile accelerating in a smooth tube, the free projectile, entering a tunnel (figure 7a), generates a precursor pressure wave which propagates ahead of it into the tunnel. Before the projectile is fully inside the tunnel, formation and propagation of this precursor wave is completely determined by the average air flow and pressure history at the tunnel entrance. After the projectile nose has fully entered the tunnel, the precursor wave is then further modified by the conditions of the air adjacent to the moving projectile face. The conditions at the projectile face, at this point, are determined by only the instantaneous projectile velocity inside the tunnel. Although the projectile entrance into the tunnel is accompanied by a very complex transitional air flow in the vicinity of the projectile nose, the problem need be considered only so far as it affects the air flow into the tunnel.

(U)   A free subsonic projectile, moving at constant velocity through the air medium, displaces the air in front of it. At any given time, the displaced air flows along a complex path, away from the projectile nose and toward the projectile base. In this respect the projectile nose may be considered the source of air flow. The average frontal projectile pressure is generally low, 3 psi being typical for subsonic projectiles. Farther from the projectile nose the air pressure varies approximately inversely with distance. Thus, the air flow and pressure more than several calibers away from the free projectile nose may be considered insignificant, at least when compared to the air flow and pressure developed by the same projectile in a smooth tube. From this it may be deduced that when a short nosed projectile enteres a tunnel, the transition of pressure from ambient to maximum at the tunnel entrance occurs in a very short time (the order of that required for projectile to traverse a distance of half its diameter).

15

(a)

(b)
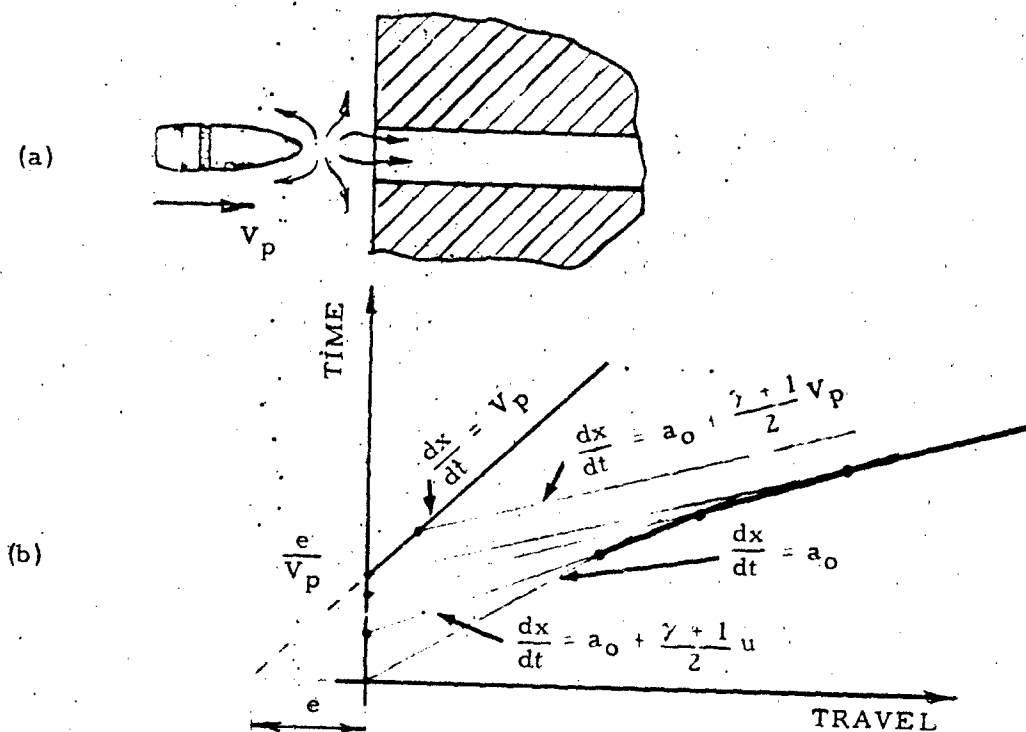
Figure 7. (U) Projectile Entering a Tunnel and the
Corresponding Precursor Travel-Time
Diagram

(U)   Generally, the nose of a small arm projectile is at least several
calibers long. As such, a more accurate representation than above may
be realized by looking at the projectile nose as consisting of a series of
point air flow sources distributed uniformly along its length. With this
representation the pressure transition from ambient to maximum at the
tunnel entrance would be expected to occur approximately in the time it
takes the projectile to traverse a distance of its nose length. The ac-
curacy in this assumption is increased with a longer projectile nose.
The projectile nose shape, although expected to affect somewhat the
pressure transition time, for present purposes can be neglected.

16

(U)   For the purposes of estimating the precursor wave generated by the projectile entering a tunnel, the following may be assumed:

1.   The time duration between the start of air flow and full projectile entrance into the tunnel is

$$t_1 - t_2 = 1/V_p \tag{24}$$

where 1 is projectile nose length and V_p is projectile velocity.

2.   During the above time duration, t_1 to t_2, the air flow velocity at the tunnel entrance varies linearly with time, i.e.

$$u = \left(\frac{V_p}{t_2 - t_1}\right)\left(t - t_1\right) = \frac{V_p^2}{1}\left(t - t_1\right) \tag{25}$$

(U)   Taking now the tunnel entrance and the start of air flow there (at time, t_1) as the zero travel and zero time reference coordinates, the air flow velocity at the tunnel entrance (from Equation 23) is

$$u = \frac{V_p^2}{1} t \tag{26}$$

for the time interval, $0 < t < 1/V_p$. The corresponding air pressure at the tunnel entrance becomes

$$P = P_o \left[\frac{a_o + \frac{\gamma - 1}{2} \frac{V_p^2}{1} t}{a_o}\right]^{2\gamma/\gamma - 1} \tag{27}$$

The propagating velocity of any given pressure magnitude in the tunnel (Equation 3) is

$$V = a_o + \frac{\gamma + 1}{2} \frac{V_p^2}{1} t \tag{28}$$

17

(U)   Thus, prior to full projectile entrance into the tunnel, the stationary tunnel entrance can be considered as the precursor pressure generating source. After the full projectile entrance into the tunnel, reference can be made to the conditions at the moving projectile face. This allows construction of the travel-time diagram for the projectile and the complete precursor wave inside the tunnel (figure 7b).

SOLUTIONS OF TYPICAL SUBSONIC SMALL ARM SYSTEM

(U)   The methods and assumptions developed above were used in calculating the precursor wave histories of various representative subsonic small arm systems. Figures 8 through 14 summarize this calculated data and other relevant information for four conventional (.22 Cal., .30 Cal., 9mm, and .45 Cal.) and two unconventional (XM76 and XM202) weapons. All precursor wave histories are presented in the pressure-travel coordinates and include the following: (1) instantaneous projectile face pressure, (2) instantaneous precursor shock pressure, (3) instantaneous pressure ahead of the precursor shock, and (4) precursor wave pressure distribution at given times and barrel locations. The plots were carried out only up to the time when the precursor shock exits from the barrel muzzle. After the shock exits from the muzzle, a rarefaction wave travels from the muzzle into the barrel, and thus establishes reverberations and a generally more complex pressure distribution in the precursor wave.

A.   Conventional .22 Cal., .30 Cal., 9mm, and .45 Cal. Weapons

(U)   Calculated precursor wave data (figures 8 through 11) indicates that each of the four weapons develops a strong precursor shock. The 9mm develops this shock the earliest, in only 3.4 inches of the barrel. The shock, when starting at 3.4 inches, is 9 psi but increases to 40 psi at 9.0 inches. The .30 Cal. develops the precursor shock latest, at 12.8 inches. This shock, when starting is only 2 psi, however, it grows to 18 psi at 22 inches of the barrel. The contrast between the .30 Cal. and the 9mm data corresponds to the peak accelerations of the two systems. Of the four weapons the peak acceleration is lowest in the .30 Cal. (1.1×10^6 ft/sec^2) and highest in the 9mm (6.5×10^6 ft/sec^2).

18
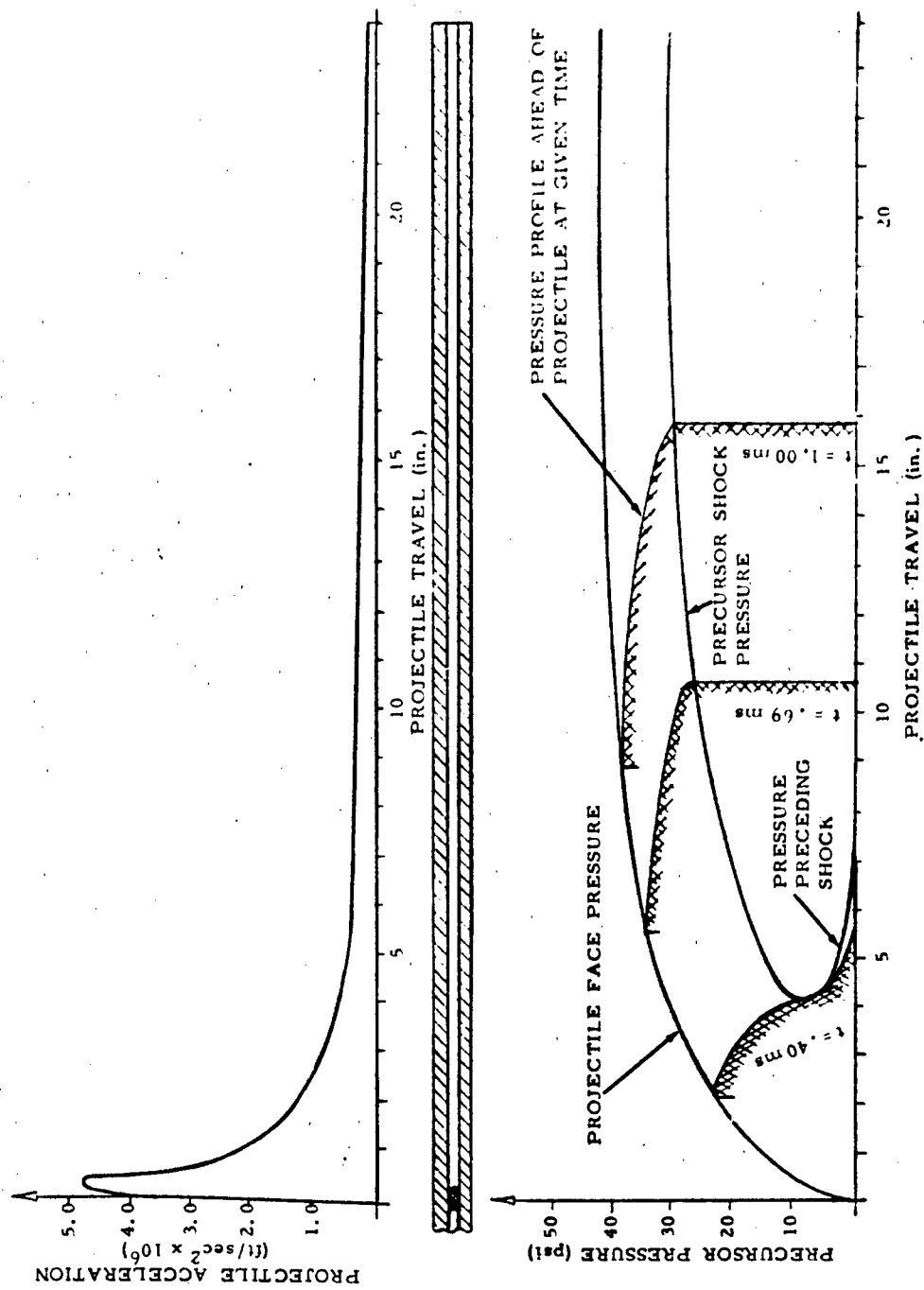
Figure 8. (U) Precursor Shock Effect for .22 Cal. Short Cartridge
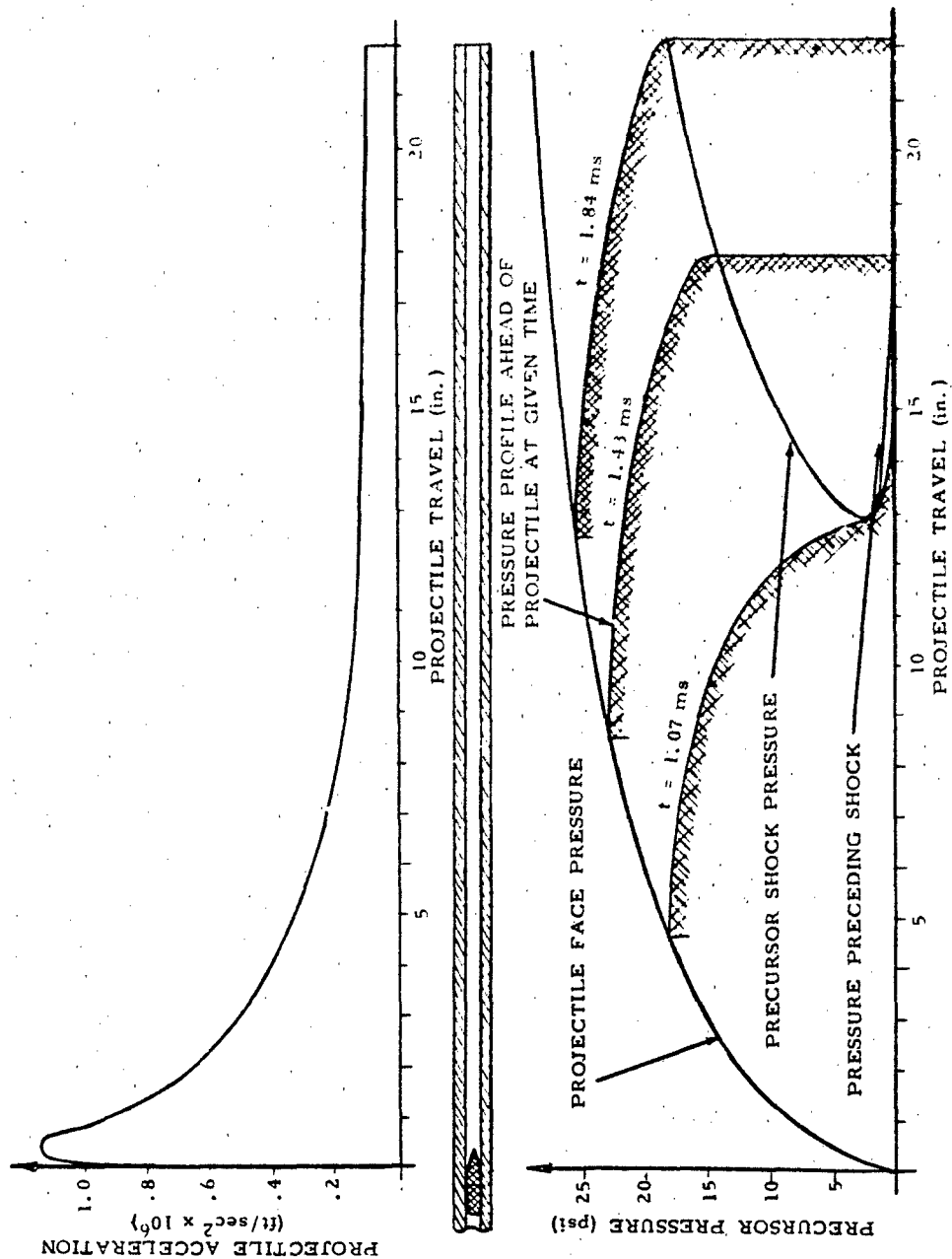
Figure 9. (U) Precursor Shock Effect for .30 Cal. (M1 Rifle) Cartridge, Special Charge.

20
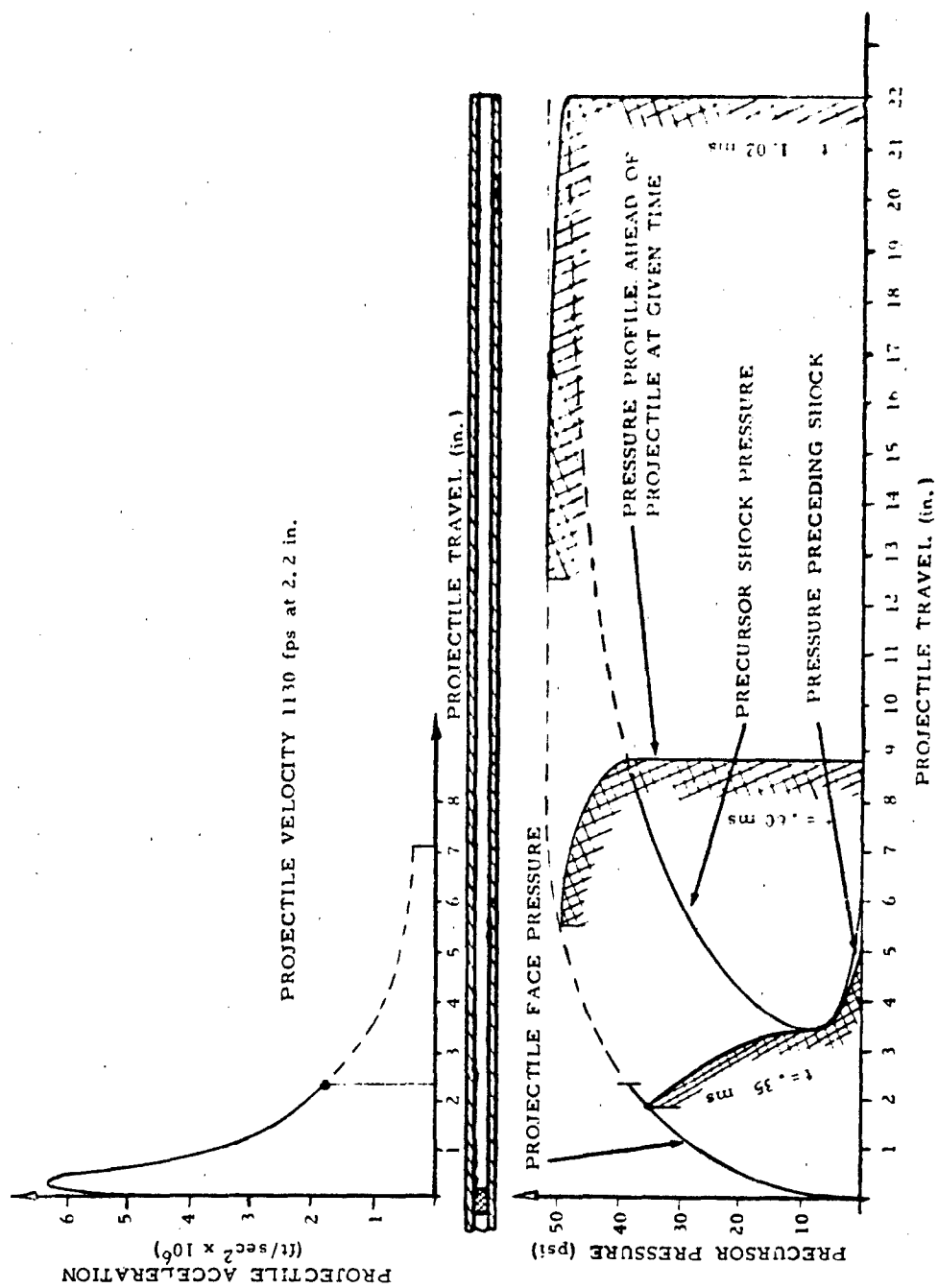
Figure 10. (U) Precursor Shock Effect for 9mm Parabellum Cartridge

21
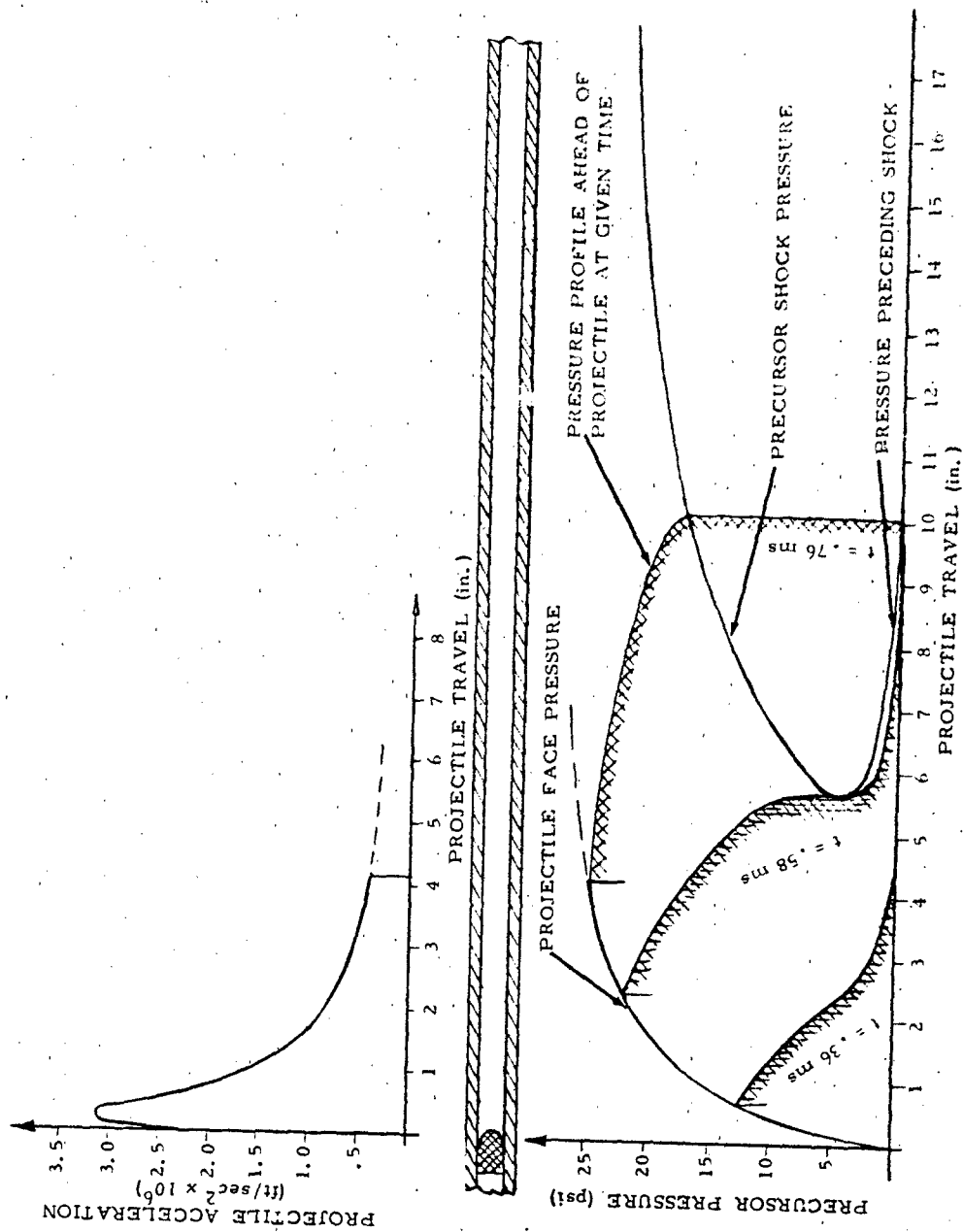
Figure 11. (U) Precursor Shock Effect for .45 Cal. M1911 Ball Round

(U)   The shaded regions in the figures represent the pressure dis-
tribution in the precursor wave at certain given times.   These times
were chosen to show the precursor wave length, magnitude and pres-
sure distribution changes with time and travel.

(U)   The dotted lines in figure 10 represent the region where the 9mm
projectile is supersonic.   The calculations for this barrel length were
carried out for general interest only.   Supersonic projectiles, due to
their ballistic crack, are of little practical value in low signature
weapons.

(U)   In general, the most significant conclusions that can be drawn
from the precursor wave data for the above four weapons are (1) the
early formation and the high initial pressure of the precursor shock
seem to depend primarily on high peak projectile acceleration and (2)
the exiting precursor shock pressure is, generally, of the order of
several atmospheres in magnitude.

B.   XM76 Cartridge (.30 Cal.)

(S)   The XM76 system (figure 12) is characterized by a very short
stroke, high acceleration and free projectile travel throughout most of
the barrel.   The projectile is accelerated by a piston which stops, after
approximately one inch of travel, leaving the projectile to coast down
the barrel.   Thus, unlike the previously described systems, the XM76
projectile actually undergoes a slight deceleration in the barrel due to
friction.   However, since the drop in velocity is fairly small (approxi-
mately 30 fps in 22 inch barrel), it was assumed that the projectile face
pressure does not decrease along the barrel after the projectile reaches
its terminal velocity at the end of the power stroke.

(S)   As seen from figure 12, the precursor shock in the XM76 sys-
tem first develops in the barrel at 1.8 inches.   It starts with 8 psi and
rapidly increases in strength until at 5.3 inches it is 24.5 psi.   The
shock remains at this final pressure for the remainder of barrel travel.
The projectile face pressure develops faster than the shock pressure,
reaching its maximum strength of 24.5 psi in 1.3 inches.   Beyond this
point the projectile face pressure remains approximately constant.

Figure 12. (S) Precursor Shock Effect for .30 Cal. XM76 System (U)

C. XM202 Cartridge (.38 Cal.)

(S)   The XM202 system with its projectile velocity and acceleration curves are shown in figure 13.   Here, as in the XM76 cartridge the projectile is driven by a piston which stops at the forward end of the cartridge.   From this point the projectile continues its travel in the barrel at approximately constant velocity.   The barrel friction velocity drop (40 fps in 13 in. barrel) for present pruposes was neglected.

(S)   Development of the XM202 precursor depends on projectile travel in three distinct areas: (1) the oversized cartridge section, (2) the cartridge discontinuity, and (3) the barrel section. If reflections at the discontinuity are neglected, the complete precursor wave may be described very simply by the equations developed earlier for each individual area.

(S)   When constructing the travel-time diagram for the XM202 projectile and its precursor wave characteristics (figure 13c), the actual projectile history is taken.   Until the projectile is one nose length from the discontinuity (at time, $t_{2,3}$), the projectile face is considered as the precursor pressure source.   The pressure magnitude (average across the oversized cartridge diameter) and the propagating velocity are specified by Equations 22 and 23.   While the projectile is within one nose length from the cartridge discontinuity, the stationary discontinuity is taken as the source of precursor pressures.   The air flow velocity at the discontinuity, for the time interval ($t_{2,3} < t < t_4$), is

$$ u = \left[\frac{V_{P4} - V_{P1}\left(\frac{A_p}{2A_t - A_p}\right)}{(t_4 - t_{2,3})} \right] t \; + \; \left[\frac{V_{P4}\, t_{2,3} - V_{P1}\left(\frac{A_p}{2A_t - A_p}\right) t_4}{(t_4 - t_{2,3})} \right] \tag{29} $$

where $t_{2,3}$ and t_4 are times when projectile is respectively one nose length from and at discontinuity, V_{P4} is projectile velocity at discontinuity, and $V_{P1}(A_p/2A_t - A_p)$ is the flow velocity at discontinuity at time $t_{2,3}$.   With the instantaneous flow velocity given, the instantaneous precursor pressure magnitude and propagating velocity at the discontinuity are specified by Equations 3 and 4b.   After the projectile nose passes the discontinuity (at time, t_4), the total precursor wave is

25
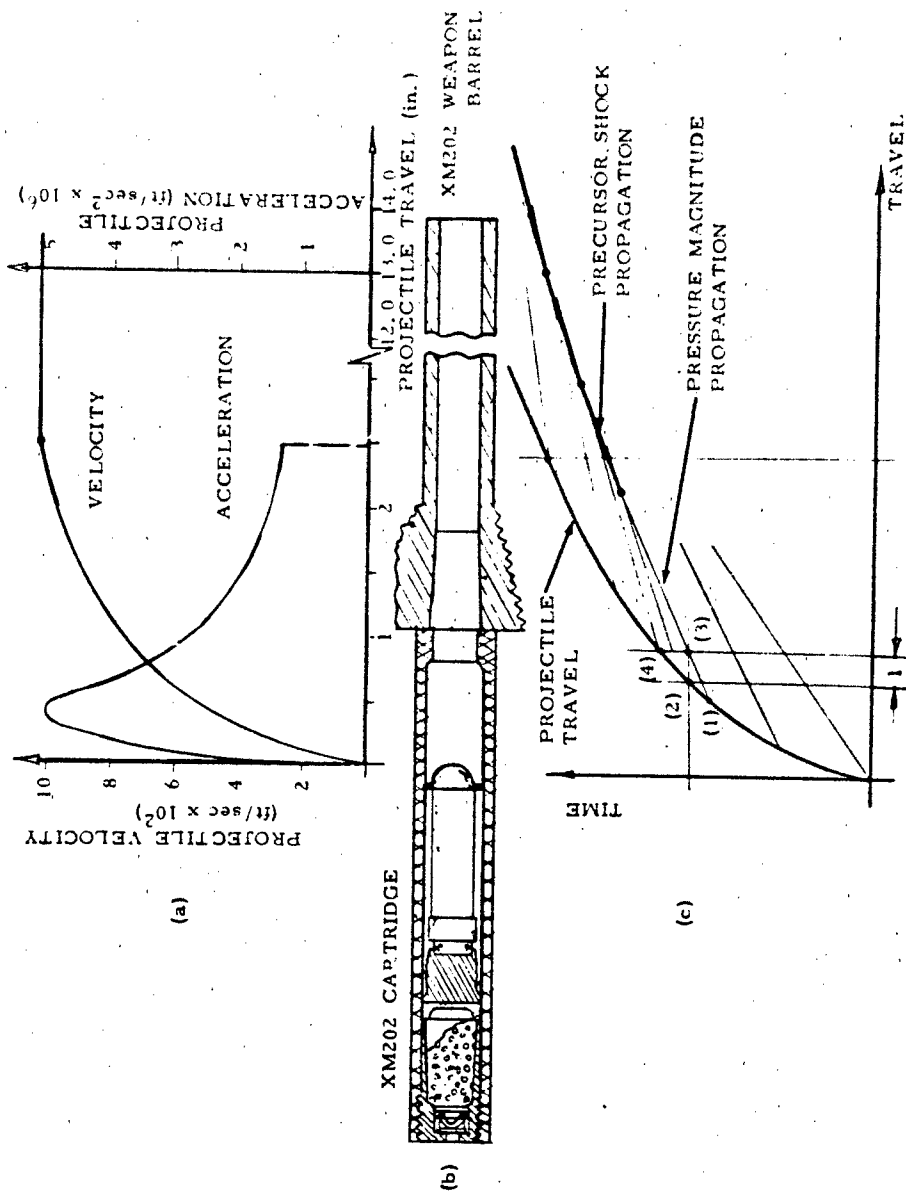
Figure 13. (S) XM202 System Configuration, Ballistics and Corresponding
Precursor Travel-Time Diagram (U)

26

modified by the instantaneous conditions at the moving projectile face. Here, the flow velocity, pressure and propagating velocity are respectively

$$V_p, \quad P_o \left[\frac{a_o + \frac{\gamma - 1}{2} V_p}{a_o} \right]^{2\gamma/\gamma - 1}$$

and

$$\left(a_o + \frac{\gamma + 1}{2} V_p \right)$$

(S)   Figure 14 shows the calculated XM202 precursor wave history in the weapon barrel. As can be seen, the XM202 precursor shock develops 1.9 inches from the initial projectile face location. The pressure of the shock when just formed is 17 psi. After the initial formation, the shock develops rapidly to 32 psi (at 9 inches). The projectile face pressure develops to 32 psi in only 2.5 inches of travel. Beyond this point the face pressure remains constant (at 32 psi) until arrival of the shock reflection (a rarefaction) from the muzzle.

APPROXIMATE PRECURSOR SHOCK SOLUTION

(U)   The above methods for computing the precursor shock are adequate for analyzing existent subsonic systems. However, they are not particularly usable for parametric studies or as guides in designing systems with desired precursor effects. This is primarily because in such cases the complete projectile base pressure and travel histories are generally not available. The usually available system data are the dimensions, weights, propellant properties and the measured or estimated peak internal pressure. This information alone, as will be shown, can yield a reasonably accurate estimate of the precursor shock formation.
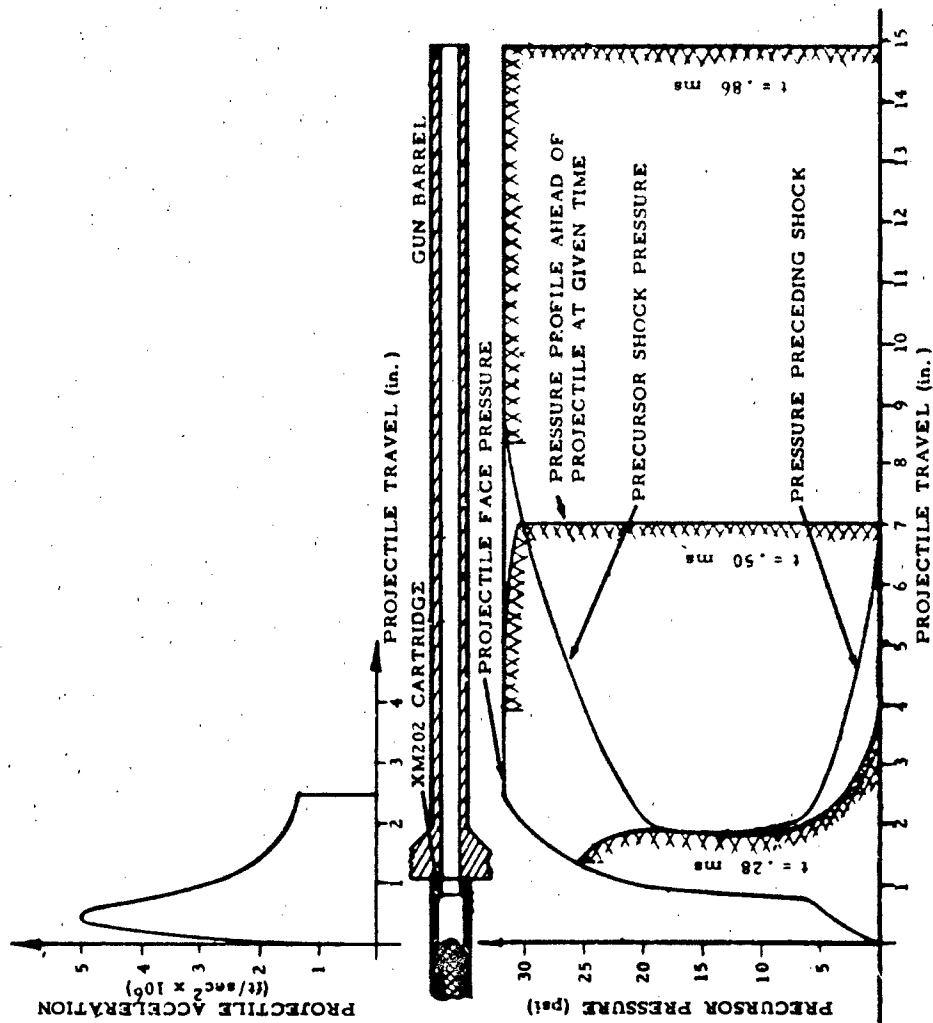
Figure 14. (S) Precursor Shock Effect for .38 Cal. XM202 System (U)

28

(U)   The location where the precursor shock first forms in a gun barrel is given by:

$$X_o = \left\{ \frac{2a_o^2}{\gamma + 1} \left[\frac{1 + \gamma M}{\dfrac{dV_p}{dt}} \right] + x \right\}_{Min} \qquad (30)$$

(U)   If the ballistic system under consideration has typical accleration, velocity and travel histories, then Equation 30 can be approximated by

$$X_o = \left\{ \frac{2a_o^2}{\gamma + 1} \left[\frac{1 + \gamma K_1 M_1}{K_2 \left(\dfrac{dV_p}{dt} \right)_1} \right] + K_3 x_1 \right\} \qquad (31)$$

where K_1, K_2, and K_3 are empirical constants and M_1, $(dV_p/dt)_1$ and X_1 are projectile Mach. No., acceleration and location respectively during peak projectile base pressure. The appropriate values for the empirical constants are given by

$$K_1 = .79$$

$$K_2 = .97$$

$$K_3 = .78$$

which were found statistically.

(U)   The location of the projectile at peak base pressure[12] is given by

$$x_1 = \left(\frac{v_o - v_c}{A_p} \right) \left[\left(\frac{2k}{k + 1} \right)^{2/k-1} - 1 \right] \qquad (32)$$

29

where v_0 is the total initial propellant chamber volume, v_c is the propellant volume, A_p is the projectile cross sectional area, and k is the propellant ratio of specific heats (~ 1.2).

(U)   The peak projectile acceleration occurs at peak pressure and is found from

$$\left(\frac{dV_p}{dt}\right)_1 = \frac{A_p P_1}{m} \tag{33}$$

where P_1 is the peak internal pressure and m is the projectile mass.

(U)   There is no simple method for determining the projectile Mach No. during peak internal pressure, however, a reasonable approximation can be made by assuming that the pressure behind the projectile varies linearly with time. Then the peak projectile Mach No. will be given by

$$M_1 = \frac{1}{a_0} \sqrt{\frac{3A_p P_1 x_1}{2m}} \tag{34}$$

(U)   By combining Equations 31 through 34 the precursor shock is found to first form in the gun barrel at

$$X_0 = \frac{2a_0^2}{\gamma+1} \left\{ \frac{1 + K_1 \gamma \left[\left(\frac{2k}{k+1}\right)^{2/k+1} - 1\right]^{1/2} \left[\frac{v_0 - v_c}{A_p}\right]^{1/2} \left[\frac{3A_p P_1}{2a_0^2 m}\right]^{1/2}}{K_2 \frac{A_p P_1}{m}} \right\}$$

$$+ K_3 \left(\frac{v_0 - v_c}{A_p}\right) \left[\left(\frac{2k}{k+1}\right)^{2/k-1} - 1\right] \tag{35}$$

a closed form solution. As can be seen, Equation 35 is usable not only for predicting the locations of precursor shock formation in a given weapon, but also for determining the system parameters affecting the early precursor shock formation.

(U)   Table I presents the calculated locations of shock formation in the six previously considered weapons. For comparison are tabulated the values predicted by Equation 35 and the values calculated from the actual experimental ballistic histories. The results in each case except the .30 Cal. indicate that a relatively small error is incurred by using the closed form solution.

Table I. (S) CALCULATED PRECURSOR
SHOCK FORMATION (U)

	X_o, Per Eq. 30 & Actual Ballistic History (Inches)	X_o, Per Eq. 35 (Inches)	% Error of Eq. 35
.22 Caliber	4.50	4.14	8.0
.30 Caliber	12.80	18.20	42.0
9 mm	3.38	3.41	.9
.45 Caliber	5.55	6.12	10.3
XM76	1.82	1.83	.6
XM202*	4.28	4.74	10.8

*Piston and smooth tube, XM202 projectile travel history.

(U)   The relatively high discrepancy in the .30 Cal. is caused by the system's somewhat unusual ballistic history. The .30 Cal. cartridge was originally derived from a standard supersonic round by reducing the propellant charge. This resulted in a larger free propellant chamber volume and a near shot-start projectile acceleration. The shot-start acceleration, in turn, introduced a substantial error in Equation

32 and, consequently, in the estimate of shock formation. Compensation for shot-start conditions in Equation 32 naturally can be expected to produce more accurate results.

(U)   The absolute pressure of the initially formed shock can be obtained from Equation 14,

$$P_{s_o} = P_o \left(\frac{a_o + \frac{\gamma - 1}{2} V_{p_o}}{a_o} \right)^{2\gamma/\gamma - 1}$$

where V_{p_o} is the projectile velocity when the initial shock pressure was generated. But from Equations 30 through 32,

$$V_{p_o} \approx K_1 a_o M_1 = K_1 \sqrt{\frac{3AP_1 x_1}{2m}} \tag{36}$$

Thus the absolute pressure of the initial precursor shock becomes

$$P_{s_o} = P_o \left\{ \frac{a_o + \frac{\gamma - 1}{2} K_1 \sqrt{\frac{3P_1}{2m} \left(v_o - v_c \right) \left[\left(\frac{2k}{k+1} \right)^{2/k - 1} - 1 \right]}}{a_o} \right\}^{2\gamma/\gamma - 1} \tag{37}$$

32

FAR FIELD SOUND PRESSURE LEVELS

A. Precursor Wave Exit From Gun Muzzle

(U)   The near sound field of the precursor wave emerging from the gun muzzle is very complex. This is so to the extent that even when problems of directivity, stagnation effects, resonant transients, and microphone reliability are surmounted, the valid data obtained is easily misinterpreted and misapplied. The far field sound effects, fortunately, besides being somewhat simpler are also generally more important in designing certain weapons for low noise output. The following is a brief description of and the method for estimating the precursor wave sound pressure levels and time durations in the far field.

(U)   Emergence of a shock-preceded precursor wave from the gun barrel, or, in general, an instantaneous air discharge from a pressurized tube is always accompanied initially by a positive sound pressure pulse. This pulse is usually of a saw-tooth form, with an almost instantaneous pressure rise followed by an exponential pressure decay with time. Since the pulse wave-length is normally many times greater than the tube diameter, acoustically the tube exit may be considered as a simple point source[3,4]. Although in near field this assumption may prove misleading, in far field it becomes useful in estimating the actual sound conditions.

(U)   For a stationary simple acoustical point source[7,8], the pressure field is given by

$$P = \frac{\left(\dfrac{d^2 m}{dt^2}\right)}{4\pi r} \tag{38}$$

where $(d^2 m / dt^2)$ is the change in air mass flow rate with time at the sound source and r is the distance to the sound source. Although Equation 38 is not directly applicable to the problem under consideration, it allows two very important conclusions. These are that (1) the instantaneous sound pressure is directly proportional to the time change in mass flow and (2) the instantaneous mass flow is directly proportional to the area under the pressure-time history of the sound signature.

33

Assuming an acoustical similarity exists between the simple source and the discharging tube, it thus becomes necessary to know the complete air flow history at the tube exit.

(U)   A simple precursor wave pressure distribution along the gun barrel is depicted in figure 15a. The conditions here are those just prior to the precursor shock reaching the barrel muzzle. For convenience, the pressure (P_1) between the projectile and the shock is assumed constant throughout. As such, the air throughout the precursor pressure column is traveling at the velocity (u_1) of the projectile (V_{p_1}). The shock velocity, of course, is supersonic.
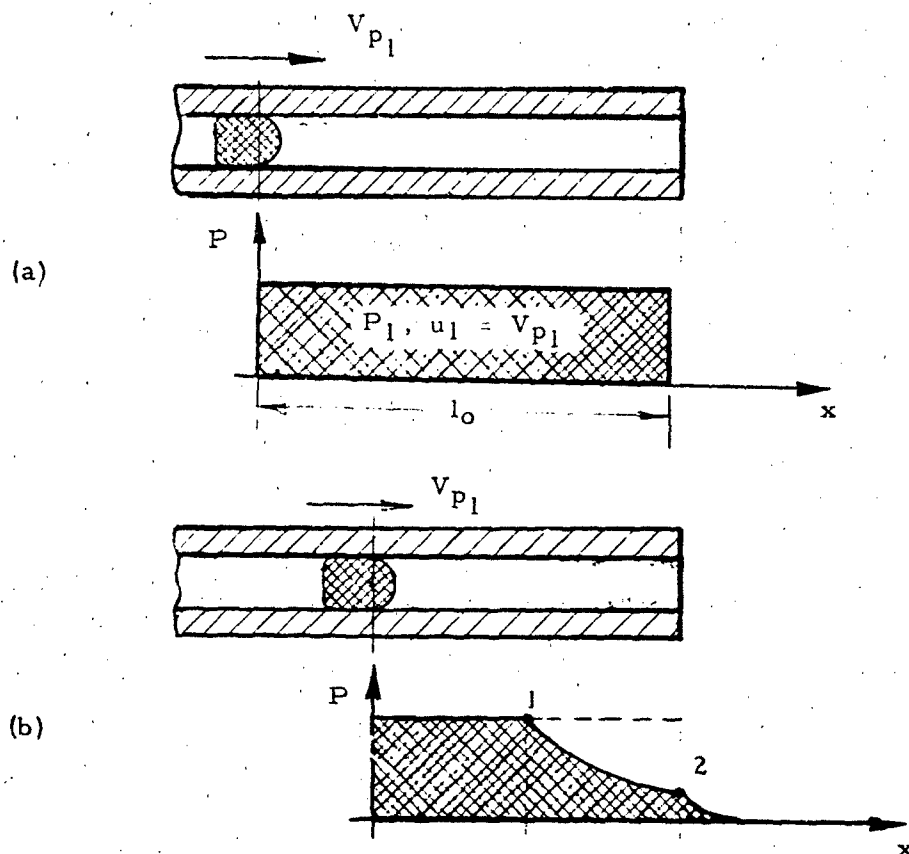
Figure 15. (U) Precursor Wave Pressure Distribution Along the Gun Barrel

34

(U)   When the shock reaches the barrel exit (figure 15b), a rare-
faction wave starts traveling from the exit back into the barrel.[9] The
rarefaction head (pt. (1)) propagates into the barrel at a velocity given
by,

$$V_r = a_o - \frac{3 - \gamma}{2} V_{P_1} \tag{39}$$

The time it takes, pt. (1), to reach the projectile (which travels at con-
stant velocity, V_1) is given by

$$t_r = \frac{l_o}{a_o + \frac{\gamma - 1}{2} V_{P_1}} \tag{40}$$

where l_o is the precursor pressure column length ahead of the projec-
tile just prior to shock exit.

(U)   In the time t_r the projectile covers a distance of,

$$l_r = \frac{l_o V_{P_1}}{a_o + \frac{\gamma - 1}{2} V_{P_1}} \tag{41}$$

(U)   After the precursor shock emerges from the barrel and before
the ingoing rarefaction (pt. (1)) returns (reflecting from the projectile),
two conditions are possible at the muzzle (pt. (2)). If the pressure of
the exiting precursor wave is

$$P_1 \leq P_o \left(\frac{\gamma + 3}{4} \right)^{2\gamma/\gamma - 1} \approx 1.95 \, P_o$$

then

$$P_2 = P_o \tag{42a}$$

$$u_2 = \frac{4a_0}{\gamma - 1} \left[\left(\frac{P_1}{P_0} \right)^{(\gamma-1)/2\gamma} - 1 \right] \qquad (42b)$$

$$\rho_2 = \rho_0 \qquad (42c)$$

and

$$a_2 = a_0 \geq u_2 \qquad (42d)$$

Equations 42a through 42d give respectively pressure, velocity, density and sonic velocity of air at pt. (2). The barrel muzzle in this case behaves as a subsonic nozzle (i.e., $a_2 \geq u_2$).

(U)   If the pressure of exiting precursor wave is

$$P_1 \geq P_0 \left(\frac{\gamma + 3}{4} \right)^{2\gamma/(\gamma-1)} \approx 1.95 \, P_0$$

then

$$P_2 = P_0 \left\{ \frac{2}{\gamma + 1} + \frac{4}{\gamma + 1} \left[\left(\frac{P_1}{P_0} \right)^{(\gamma-1)/2\gamma} - 1 \right] \right\}^{2\gamma/(\gamma-1)} \qquad (43a)$$

$$u_2 = \frac{2a_0}{\gamma + 1} \left[2 \left(\frac{P_1}{P_0} \right)^{(\gamma-1)/2\gamma} - 1 \right] \qquad (43b)$$

$$\rho_2 = \rho_0 \left(\frac{P_2}{P_0} \right)^{1/\gamma} \qquad (43c)$$

and

$$a_2 = \frac{2a_0}{\gamma + 1} \left[2 \left(\frac{P_1}{P_0} \right)^{(\gamma-1)/2\gamma} - 1 \right] = u_2 \qquad (43d)$$

36

In this case the barrel muzzle behaves as a supersonic nozzle (i.e., $a_2 = u_2$). This supersonic condition is typical with precursor pressures generated by the projectile traveling at higher velocities than $a_o/2$.

(U)   Assuming that the muzzle air flow is supersonic (Equation 43 holds), the time it takes for the ingoing rarefaction (pt. (1)) to return to the muzzle (reflecting from the projectile) is

$$ t_e = l_o \frac{\left(\dfrac{V_{P_1}}{\dfrac{2}{\gamma + 1} a_o + V_{P1}} \right)^{(\gamma + i)/4}}{\left(a_o + \dfrac{\gamma - 1}{2} V_{P1} \right)} \tag{44}$$

(U)   After the precursor shock exits and before the reflected rarefaction returns to the barrel muzzle (at time, t_e), the air mass outflow from the muzzle is governed by Equation 43 and is

$$ \dot{m}_m = \rho_2 u_2 A_t \tag{45}$$

(U)   After the return of the rarefaction, the air pressure and air density at the muzzle (pt. (2)) begin to decrease. When finally the projectile emerges at the muzzle, the conditions at the muzzle are approximately atmospheric and the velocity of air outflow is that of the projectile. After emergence of the rarefaction and before the emergence of the projectile, the air outflow from the gun muzzle, to the first approximation, may be assumed to decrease linearly.

(U)   The time lag between exits of the precursor shock and the projectile is

$$ t_p = l_o / V_{P_1} \tag{46}$$

(U)   Thus, above equations describe completely the precursor air mass flow history at the gun muzzle. Figure 16a shows this flow history up to the time when projectile exits from the barrel.

PRECURSOR AIR MASS OUTFLOW HISTORY
AT GUN MUZZLE

(a)

PRECURSOR
SHOCK EXIT

RAREFACTION EXIT

PROJECTILE EXIT

(b)

SOUND PRESSURE HISTORY IN FAR FIELD
PERPENDICULARLY FROM GUN MUZZLE

P_m

P_n

T

t_e

t_p
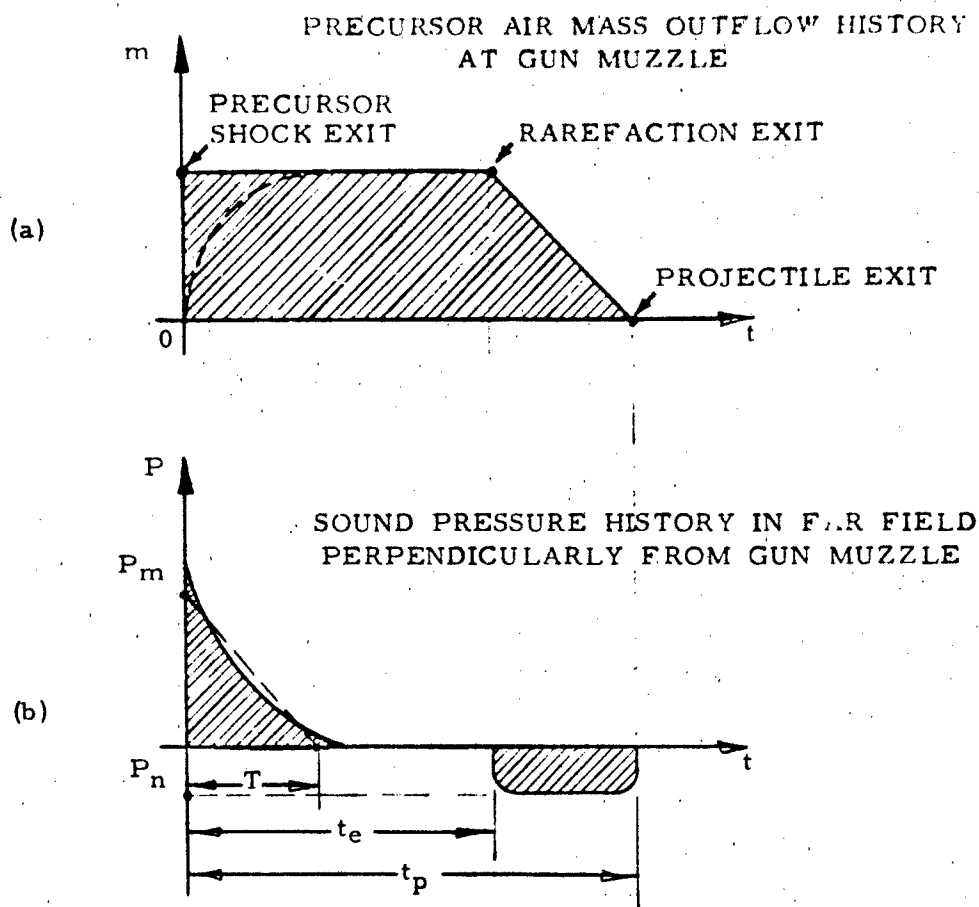
Figure 16. (U) Precursor Air Mass Outflow History and
Sound Pressure History

(U)   Now, from description of the mass flow at the gun muzzle and
Equation 38, it is possible to make certain conclusions in reference to
the precursor sound pressure in the far field. Due to the air mass flow
of figure 16a, what would be expected initially is an extremely high sound
pressure of very short duration. However, since this lacks support in
actuality, more consideration must be given to the empirical data and
the limitations of Equation 38.

(U)   The experimental data on discharging tubes indicate that the initial precursor sound pulse can be depicted as shown in figure 16b. Comparing this pulse to the corresponding mass flow of figure 16a, it is seen that their relationship is somewhat complex. However, keeping in mind the limitations of the previously assumed point source, the initial mass discharge in figure 16a can be modified (for computational purposes) to that shown by the broken line. The precursor pulse can be adequately represented by the saw-tooth formed by the broken line of figure 16b.

(U)   The fundamental frequency[13] of a steadily discharging jet is defined by the empirical constant,

$$k = fd/u \tag{47}$$

Here a typical value of k is .13, u is the jet flow velocity and d is the jet diameter.

(U)   Using the above equation, the time duration of the simplified positive sound pulse of figure 16b is

$$T \approx d/2ku_2 \tag{48}$$

where d is the inside gun barrel diameter. This time duration, the straight line saw-tooth pulse configuration, together with Equation 38, yield the peak precursor sound pressure* as

$$P_m = \frac{k\dot{m}_m u_2}{\pi r d} = \frac{kd\rho_2 u_2^2}{4r} \tag{49}$$

or

$$\frac{P_m}{P_o} = \frac{\gamma k}{4r} dM_2^{2\gamma/\gamma - 1} \tag{50}$$

where M_2 is the air flow Mach No. (u_2/a_o).

---

*Since $\dot{m}_m = 4\pi r \int_0^T P dt \approx 4\pi r \dfrac{P_m T}{2}$

39

(U)   Similarly to above, the negative sound pressure due to the precursor rarefaction is given by

$$P_n \approx - \frac{\dot{m}_m}{4\pi r (t_p - t_e)}$$

(51)

where $(t_p - t_e)$ is the time duration between emergence of rarefaction head and emergence of projectile at the gun muzzle.

(U)   From the above it is seen that the peak precursor sound pressures are primarily determined by the gun caliber[10] and the maximum air mass discharge rate. The negative sound pressure, in addition, is dependent on time of the rarefaction wave return to the muzzle. Equation 51 indicates that small values of $(t_p - t_e)$ should result in a very high negative sound pressure, P_n. This would be expected in the case when the projectile velocity begins to approach the supersonic range.

(S)   In systems such as the XM76 and the XM202 the projectile base pressures in the barrel are lower than atmospheric. Because of this, further consideration must be given to the air inflow into the barrel after the projectile leaves the muzzle. Analysis of this problem is straight-forward and similar to the one described above, however, now the air flow conditions at the barrel muzzle are determined by the energy equation* rather than the wave equation. After projectile exit the initial air flow into the gun barrel is supersonic with mass flow, density and velocity at the muzzle being given respectively, by

$$\dot{m}_2 = - \rho_2 u_2 A_t$$

(52a)

$$\rho_2 = \rho_o \left[2/(\gamma + 1) \right]^{1/(\gamma-1)}$$

(52b)

and

$$u_2 = a_2 = a_o \left[2/(\gamma + 1) \right]^{1/2}$$

(52c)

---

* $a^2 + \frac{\gamma - 1}{2} u^2 = $ const.

The above conditions will persist at the exit until the reflection of the incoming wave returns from the tube breech. Generally, the peak negative sound pressure generated by this inflow is similar in magnitude to the positive portion of the precursor pulse previously described. At large distance from the gun muzzle, the typical total precursor sound pulse will tend to approximate more and more a balanced N-wave configuration, beginning with a positive and ending with negative shocks. This tendency is caused primarily by the viscous effects of air and the local sonic velocity differentials within the pulse.

(C) . In the conventional systems, unlike in the XM76 and the XM202, the projectile is driven by a high propellant gas pressure. The propellant gas flow history at the gun muzzle, following the projectile exit, is very similar to the flow history of the precursor wave (figure 16a). Immediately after uncorking of the barrel, supersonic flow conditions are established at the muzzle. This flow condition persists until the rarefaction traveling into and reflecting inside the barrel returns. The consequent sound pressure pulse in the far field is generally of the N-shape, with the initial positive and the subsequent negative pulse portions being determined respectively by the abrupt gas discharge and the eventual reflection of the rarefaction traveling into the barrel. Since the propellant gas sound pressures in this case are generally high, the sound pulse wave length can be expected to increase substantially with distance from the weapon. In all other respects analysis of the sound signature due to the propellant gas discharge can be similar to that of the precursor sound signature.

(U) Above equations (Eqs. 49, 50 and 51) for precursor sound pressures apply in the direction perpendicular to the weapon line of fire. Since the precursor air is discharging from the barrel in the forward direction, the generated sound pressures will be highest in front of the weapon and lowest behind the weapon. The sound pressures generated perpendicularly to the weapon will be between the two extremes. This directional effect can be represented by the spherical pressure field modified by the factor $(1 - (M_2/2) \cos \theta)^{-1}$, where M_2 is the air mass flow Mach No. (u_2/a_0), and θ is the azimuth angle from the line of fire.[13] The complete peak precursor sound pressure field then becomes (from Equation 49),

$$P_m = \frac{kd\rho_2 u_2^2}{4r\left[1 - (M_2/2) \cos \theta\right]} \tag{53}$$

41

(C)   The corresponding peak sound pressure level in decibels is

$$L_m = 20 \log_{10} \left\{ \frac{\left(\frac{kd \rho_2 u_2^2}{4r\left[1 - (M_2/2)\cos\theta\right]} \right) 10^6}{(.0002) P_o} \right\} \tag{54}$$

(S)   Table II lists the various calculated and measured precursor sound data for the six previously considered weapons. The calculated precursor peak sound pressure levels (SPL), and the muzzle discharge conditions were determined from the exiting precursor shock pressures taken from figures 8 through 14. From the calculated data it is seen that all weapons except the .45 Cal. discharge the precursor air at supersonic conditions. The discharge pressure and the Mach No. are highest in the XM202, corresponding to the highest exiting precursor shock pressure. The .45 Cal., because of its incompletely developed precursor shock, develops subsonic conditions at the muzzle. As such, the precursor air discharges from the muzzle at atmospheric pressure and approximately sonic velocity.

(S)   From Equation 50 it is seen that the peak precursor sound pressure is primarily determined by the weapon caliber and the discharge Mach No. The Mach No., in turn, is only dependent on the exiting precursor shock pressure. Consequently, the XM202 has the highest peak sound pressure (220×10^6 ubars) and the SPL (121 db) of the six weapons. In contrast the .22 Cal. has a fairly high exiting shock pressure (31 psi) but because of its small caliber develops a substantially lower SPL (116 db). The .45 Cal., with its larger caliber, develops a relatively low SPL (109 db at 384 inches) because of its low discharge Mach No. For comparison, Table II also shows the experimentally measured SPL of various systems. This data was obtained from scope traces similar to those shown in figures 17 and 18. In each system except the .45 Cal., the measured SPL was approximately 6 db lower than the calculated value. This discrepancy, although seemingly high at first glance, is reasonable in view of the measuring errors and calculating assumptions. The greatest probable measurement error is due to the slow microphone response to a shock wave.[11] As may be surmised from figure 17, by the time the microphone fully responds to the initial precursor shock, the pulse pressure has already dropped

42

Table II. (S) CALCULATED vs MEASURED PEAK SOUND PRESSURE LEVELS PERPENDICULARLY
FROM THE MUZZLE   (U)

	XM202	XM76	.22 Cal.	.30 Cal.	9mm	.45 Cal.
Barrel Diameter, d (in.)	.350	.310	.225	.310	.350	.450
Barrel Length, l (in.)	10.0	22.0	24.0	22.0	6.1	5.0
Exiting Shock Pressure, P_1 (psi)	32.0	24.5	31.0	18.0	30.0	13.8 [1]
Discharging Pressure, P_2 (psi) [2]	21.1	11.3	20.5	4.5	17.3	0
Discharging Mach No. [3]	1.14	1.08	1.13	1.05	1.12	1.00
Distance from Muzzle, r (in.)	181	181	181	181	181	384
Peak Sound Pressure Ratio, $\delta_m = P_m/P_o \times 10^{-6}$ [4]	220	134	133	105	193	54
Calculated Sound Pressure Level, L_m (db) [5]	121	116	116	115	120	109
Measured Sound Pressure Level, L_m (db)	115	110	-	109	-	109

(1) Shock is not yet developed in given barrel length - the effective precursor pressure of 13.8 psi was determined from Figure 11.

(2) Per Equation 43a

(3) Per Equation 43b

(4) Per Equation 50

(5) Per Equation 54

43

(a)
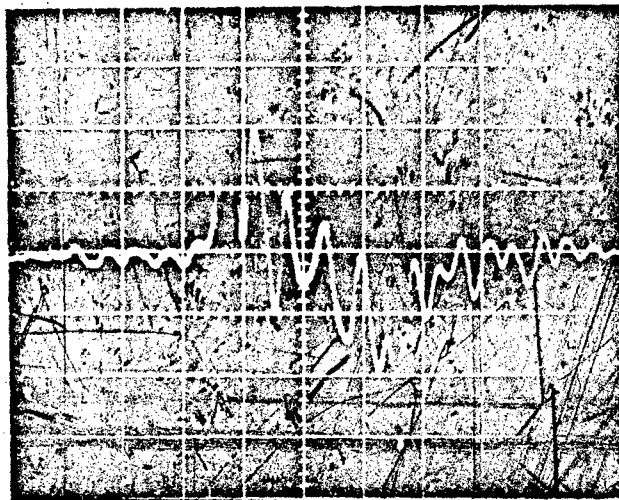
XM202 Cartridge (10" bbl) y = 28. 3 ubars/cm
15 Ft. ⊥ from Muzzle   x = .2 ms/cm
           1 cm = 1 major division

(b)
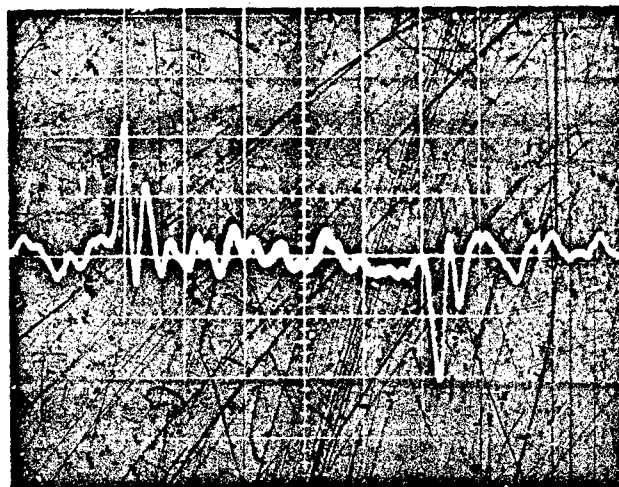
XM76 Cartridge (22" bbl) y = 28. 3 ubars/cm
15 Ft. ⊥ from Muzzle   x = .25 ms/cm
          1 cm = 1 major division

Figure 17. (S) XM202 and XM76 Precursor and Vacuum Sound
     Pressure-Time Traces (BR 150 Altec Microphone) (U)

(a)
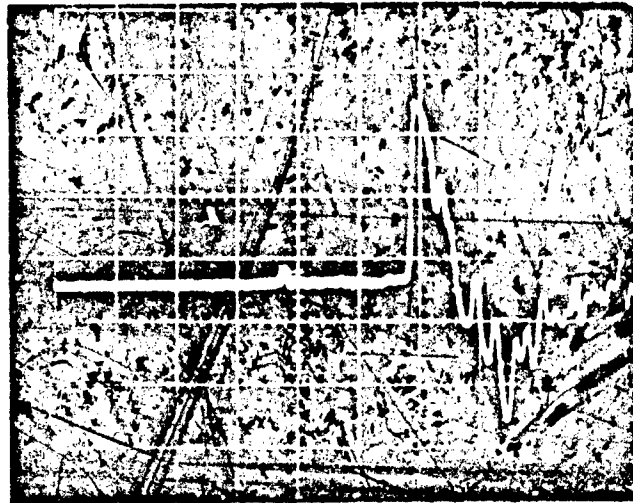
.30 Cal. Cartridge (22" bbl)   y = 258 ubars/cm
15 Ft. ⊥ from Muzzle   x = .5 ms/cm
                               1 cm = 1 major division

(b)
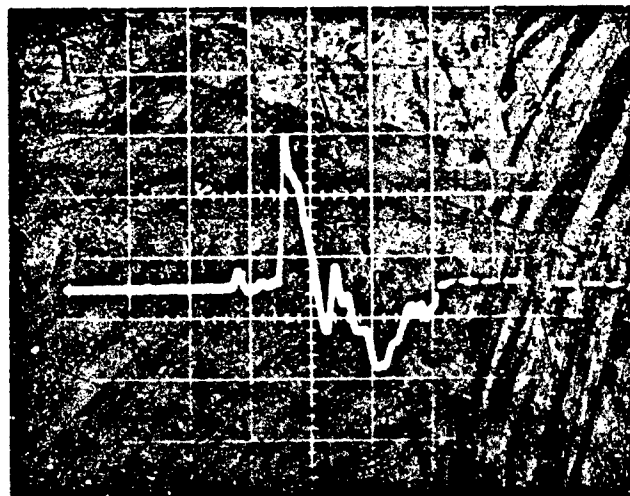
.45 Cal. Cartridge (5" bbl)   y = 227 ubars/cm
31.3 Ft. ⊥ from Muzzle   x = .5 ms/cm
                              1 cm = 1 major division

Figure 18. (U) .30 Cal. and .45 Cal. Precursor and Blast Sound
                Pressure-Time Traces (Br 150 Altec Microphone)

45

substantially. A better correlation between measured and calculated SPL is found in the .45 Cal. because of the not fully developed precursor shock and the consequent slow sound pressure pulse rise. The greatest possible calculating error is probably introduced by Equation 48. Here, the value of constant k (.13) used was based on near field data of larger jets. Better accuracy would be realized by also taking into consideration the sound pulse wave length increase with distance from the weapon. Another point of interest is the effect of outside barrel diameter and possible muzzle flanges on the far field SPL. This, however, is beyond the intended scope of this report.

(U)   Figures 17 and 18 show the sound pressure-time scope traces of the XM202, XM76, .30 Cal. and .45 Cal. weapons. The traces, although somewhat marred by the resonant frequency of the microphone, do show the positive and negative portions of the precursor pulse.

(S)   In both the XM202 and XM76 the major positive and negative sound pressures correspond to respectively the precursor shock exit from the barrel and the vacuum uncorking by the projectile. Figure 18 shows the .30 Cal. and the .45 Cal. precursor pulses as small initial pips. Immediately following these are the sound pressure signatures due to propellant gas discharge following projectile exit from the barrel.

(S)   The calculated directivity effects of the XM202 and the XM76 systems are shown in figure 19. The peak sound pressures in each case are higher in the forward direction than rearward. In each case the SPL difference between rear and front at 15 feet from the muzzle is approximately 10 db. This is probably a conservative estimate; however, no experimental data is extant for the various azimuth angles.

B.   Projectile Exit Through Flexible Baffle

(C)   It has been found that some gun silencers[1] are designed with a flexible baffle (plastic, foams, etc.) at the exit (figure 20). This baffle is such that it has a natural tendency to close off the internal silencer cavity unless forced open by high pressure gases or the exiting projectile. Although the intent and performance of this design can only be guessed, a baffle of proper rigidity can allow the projectile to pass and yet restrict substantially the gas flow due to any low internal silencer pressures. This would include the previously discussed precursor pressures and the possible propellant gas blow-by around the
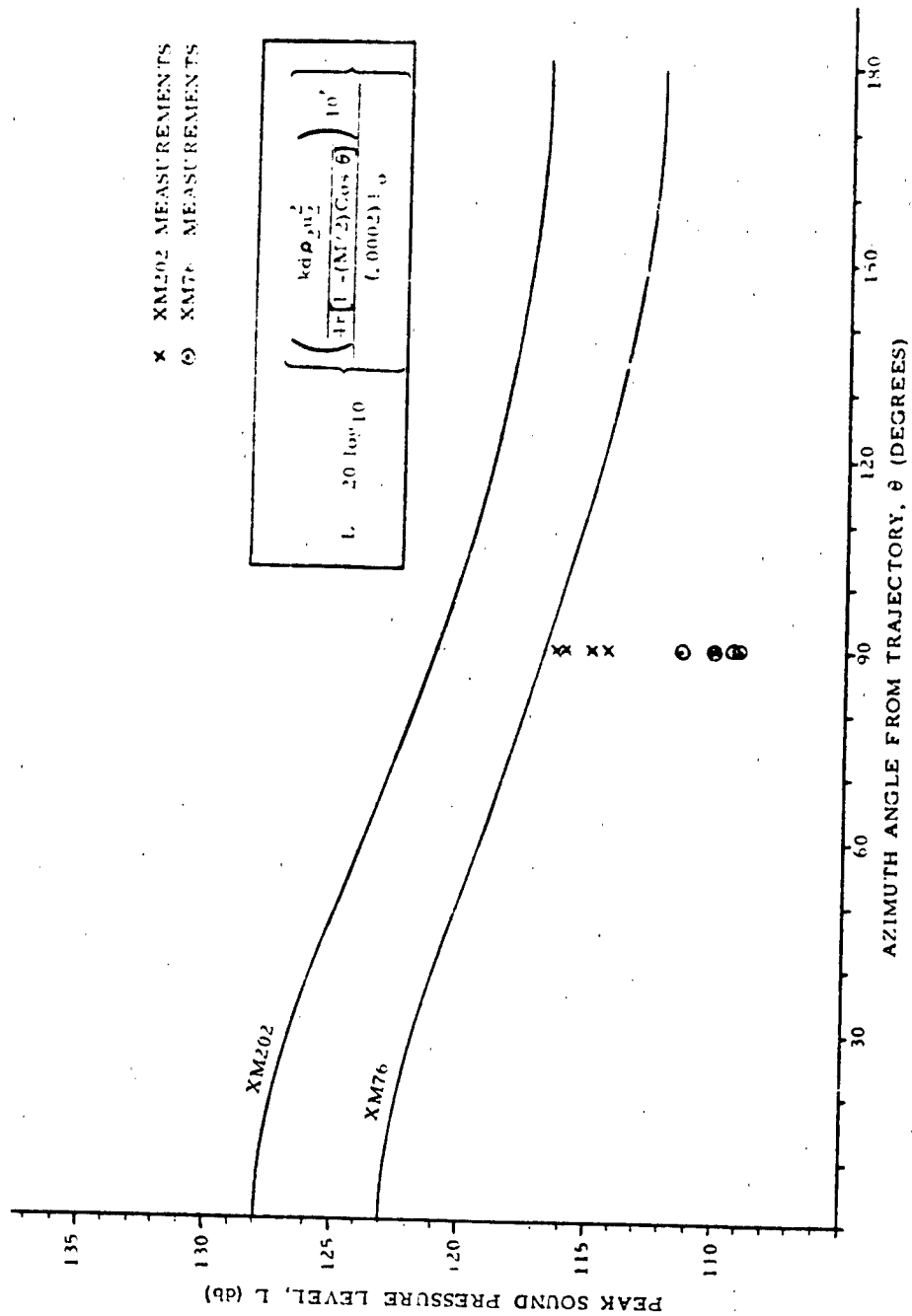
46

Figure 19. **(S)** Sound Pressure Levels vs Azimuth Angle From Trajectory, 15 Feet From Gun (U)

47
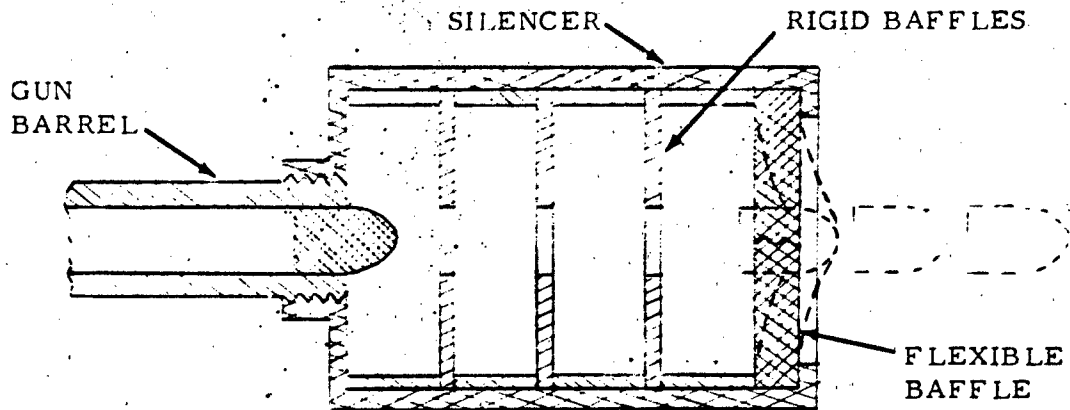
Figure 20. (U) Projectile Exit Through Flexible Baffle

projectile. Any restriction of gas flow from the silencer exit naturally results in attenuation of the far field sound pressure.

(C)   Although the flexible baffle generally tends to reduce the noise generated by the discharging gasses, the abrupt exit of the projectile through the baffle generates a noise of its own. The basic mechanism of this noise generation consists of the following: (1) when a projectile exits the gun silencer, it displaces the air particles in front of the silencer, and (2) this displacement results in air particle acceleration and, of necessity, is accompanied by a local force, pressure and, consequently, by a corresponding far field sound pressure. Since presently no experimental data is available to elucidate the above phenomenon, it may be of interest to speculate (even if boldly) on the sound pressure magnitudes to be expected from the use of a flexible baffle in silencers.

(C)   The projectile exiting through a flexible silencer baffle may be looked upon (similarly to precursor shock) as a simple acoustical source, whose boundary is the projectile surface outside the silencer. The spherical sound pressure field then can be described by

$$P = \frac{\rho_0 \, (d\overset{2}{v} / dt^2)}{4\pi r} \tag{55}$$

where $(d^2\dot{v}/dt^2)$ is the change in volume displacement rate per time, ρ_o is the atmospheric air density and r is the distance to the gun muzzle.

(C)   If a fairly blunt nosed and very long projectile is assumed, the initial sound pressure signature can be expected to be of a positive, linear saw-tooth configuration, preceded by a shock or a near-shock (figure 21).
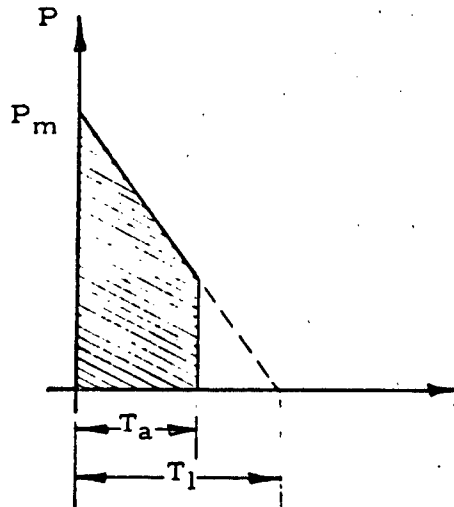
Figure 21.   (U)   Expected Sound Pressure-Time Signature of
                   Long and Short Projectiles

The period of this positive saw-tooth pulse from a long projectile (per Eq. 48) is then

$$T_1 \approx d/2kV_p \qquad\qquad (56)$$

where d is projectile diameter, V_p is projectile velocity and k is an empirical constant ($\sim .13$). When the projectile exits fully from the silencer, there is a sudden cessation of air mass flow from the silencer.

49

The mass flow due to the volumetric displacement of the projectile then becomes directed from the projectile nose to the projectile base. This effect would be expected to result in an abrupt decrease of sound pressure, possibly even into the negative region. Thus the total sound pulse time duration, when limited by the projectile length, is

$$T_a = 1/V_p \tag{57}$$

where 1 is the projectile length.

(C)   Since the projectile volumetric displacement rate during exit from the silencer is

$$\frac{dv}{dt} \approx \frac{\pi d^2}{4} V_p = \frac{4\pi r}{\rho_o} \int_o^{T_1} P dt \approx \frac{4\pi r P_m T_1}{2\rho_o} \tag{58}$$

the peak sound pressure, perpendicularly from the gun, becomes

$$P_m \approx \frac{\gamma k P_o}{4r} dM_p^2 \tag{59}$$

where P_o is atmospheric pressure (14.7 psi), M_p is the projectile Mach No., and γ is air specific heat ration (~ 1.4).

(C)   Thus the peak sound pressure level generated by a projectile exiting through a flexible baffle (from Equation 58) will be expressed by

$$L_m = 20 \log_{10} \left\{ \frac{\left[\frac{\gamma k}{4r} dM_p^2\right] 10^6}{(.0002)} \right\} \tag{60}$$

50

Incorporating the directivity effect, the above equation becomes

$$L_m = 20 \log_{10} \left\{ \frac{\left(\dfrac{\gamma k d M_p^2}{4r\left[1 - (M_p/2)\cos\theta\right]} \right) 10^6}{.0002} \right\}$$ (61)

where θ is the azimuth angle from the line of fire.

(C)   For proper acoustical evaluation of a system, consideration must be given, in addition to the peak SPL, also to the sound pulse dura ions. Since the physiological response to short, transient sounds is generally very complex, an expedient qualitative comparison between two given sound pulses can be made on the basis of "effective" pulse frequency, an inverse of pulse period. For a sound pulse shown in figure 21 the effective frequency is

$$f = V_p/2l$$ (62)

(C)   Since small arm projectiles are generally designed for low flight drag, the projectile base and nose sections may be expected to have finite and tapering lengths. The consequence of this is that the sound pulse generated by the projectile exiting through a flexible baffle will have a finite pressure rise and fall (figure 21). However, since the volumetric displacement rate of the projectile is still proportional to the area under the sound pressure-time history and since the projectile nose and base lengths cannot exceed the total projectile length, the peak SPL of a streamlined projectile would not be expected to deviate by more than 6 db from that predicted by Equation 61.

(C)   The above analysis was applied to the projectiles of the six previously considered systems. The calculated sound data for these projectiles when exiting through a flexible baffle are listed in Table III. It is seen that the larger caliber projectiles traveling at higher Mach Nos. have the highest SPL values. However, all values fall within a fairly close proximity of each other. The calculated effective frequencies of various projectiles, on the other hand, have a much larger spread than the SPL values. Whereas the XM202 and .22 Cal. projectiles have practically identical peak SPL's, their frequencies are respectively 3850 cps and 25600 cps. Although the loudness of each of the two sound

Table III. (S) SOUND PULSE DATA FOR PROJECTILES EXITING THROUGH A FLEXIBLE SILENCER BAFFLE* (U)

	d (in.)	l (in.)	M	r (in.)	P_m/P_o	L_m (db)	f (cps)
XM202	.350	1.50	.85	181	63×10^{-6}	110	3850
XM76	.310	.70	.70	181	43×10^{-6}	107	6800
.30 Cal.	.310	1.00	.88	181	60×10^{-6}	110	6000
.45 Cal.	.450	.55	.71	181	57×10^{-6}	109	8800
9mm	.350	.42	1.15	181	120×10^{-6}	116	18600
.22 Cal.	.22	.27	1.02	181	50×10^{-6}	109	25600

*Perpendicularly from the weapon.

pulses is not immediately apparent, the data may be interpreted in the light of human audio sensitivity for continuous pure tones. The 25600 cps borders on the insensitive range of human hearing while 3850 cps is very much in the most sensitive portion of the frequency spectrum. From this it may be concluded that the .22 Cal. projectile would be substantially quieter than the XM202 projectile, even though their peak SPL values are almost identical.

(S) It is interesting to compare the calculated peak SPL's of projectiles exiting through a flexible silencer baffle (Table III) with the measured peak SPL's of projectiles in free flight. The calculated SPL of the supersonic 9mm projectile exiting the silencer is 116 db. The XM202 projectile in free flight (at Mach No. of .85) generates approximately 87 db at 181 inches from trajectory. In contrast, the ballistic crack of a typical supersonic projectile is of the order of 150 db, and varying little with projectile Mach No. and caliber. The seeming lack of correlation between various data is resolved by the fact that the sound of both the exiting projectile and the free subsonic projectile spreads spherically, while the sound of ballistic crack spreads cylindrically. Consequently, the sound pressure of the former two projectiles attenuates inversely with distance ($P \propto r^{-1}$) and that of the latter attenuates inversely with distance to the 3/4 power ($P \propto r^{-3/4}$).

CONCLUSIONS

(U)   In summary, a subsonic projectile traveling in the gun barrel compresses the air ahead of it. The pressure gradient and length of the precursor wave thus generated is transient, varying with time and projectile travel. In general, the pressure is highest near the projectile face and lower further down the barrel. With typical gun barrel lengths and ballistics, the precursor wave prior to exit from the gun muzzle is preceded by a shock. The shock pressure depends on the complete projectile acceleration history, while the projectile face pressure is determined by instantaneous projectile velocity. After the shock reflects from the gun muzzle, the precursor wave pressure dependence becomes more complex. Projectile face and shock pressures of 20 psi are not uncommon in small caliber subsonic weapon barrels.

(U)   When the precursor wave in front of the projectile exits from the gun muzzle and is not masked by other gun effects, it becomes the source of a relatively loud sound report. The most significant portion of this sound is the positive saw-tooth pressure pulse preceded by a shock. The peak pressure of this pulse is directly proportional to the gun caliber and the seventh power of air discharge Mach No. from the gun muzzle. The discharge Mach No., in turn, is dependent on the exiting precursor shock pressure, and is usually slightly higher than 1. The peak sound pressure level due to precursor effects in typical subsonic small arm weapons are of the order of 115 db at 15 feet perpendicularly from the gun barrel. The typical major positive precursor pulse duration is in the vicinity of .1 milliseconds.

(U)   In brief, to minimize the peak sound pressure level due to the precursor wave, the projectile caliber, velocity and peak acceleration should be as small as possible. On the other hand the projectile mass (at constant energy output), the propellant chamber volume and the propellant charge should be made large. The "shot-start" projectile acceleration naturally should be avoided since it causes an early precursor shock formation in the barrel.

(U)   Although specific experimental data is lacking, the precursor sound pressure field is expected to be directional. An estimate of this directivity for typical small arm weapons indicates that approximately a 10 db higher reading may be expected downrange than behind the gun.

53

(C)   The abrupt exit of the projectile through a flexible baffle in a
silencer generates a certain amount of noise. This can be expected
even when the projectile is not followed or preceded by high propellant
or precursor pressures. The basic mechanism of this noise generation
being similar to that of an exiting precursor pressure wave, the problem
was considered in the light of the already developed method of analysis.
Calculations indicate that a typical subsonic small arms projectile exit-
ing through a flexible silencer baffle should generate about 110 db peak
sound pressure level at 15 feet perpendicularly from the gun muzzle.
The time duration of the generated sound pulse is directly proportional
to the projectile length. A 1.5 inch long projectile exiting at Mach No.
.8 generates a sound pulse of .138 milliseconds time duration while a
.5 inch projectile exiting under the same conditions will produce a pulse
of only .046 milliseconds time duration. Because of this, the exit of
the latter is expected to be substantially quieter than the exit of its
longer counterpart.

(U)   The analytical methods presented in this report are simple, often
perhaps at the expense of accuracy. Primary effort has been directed
toward establishing a parametric dependence and a method of analysis
of noise generated by an exiting subsonic projectile. Although in cer-
tain applications the presented equations may be found insufficiently ac-
curate, for general considerations of noise produced by small arms
weapons they provide a starting point. No efforts were devoted to in-
vestigating methods of reducing the described weapon noises. However,
it was intended and hoped that the solution to this problem would become
self-evident with understanding of the physical mechanisms herein de-
scribed.

(C)   The cursory considerations of the precursor wave sound effects
revealed that analytical work in reference to attenuation of small arm
weapon noise either has not been attempted or simply has not been pub-
lished. Whatever the reason, very little material directly pertinent to
the subject is in existence. Reliable experimental data on small arm
noise likewise is scarce. This, perhaps in part, is due to only recent
advent of microphones suitable for recording shock waves.[11] In con-
trast to the above deficiencies, there exist today hundreds of gun si-
lencer patents and numerous records of successful and unsuccessful
attempts to attenuate or minimize gun noises. Irrespective of this,
the low signature weapons still remain as an unutilized military po-
tential.

54

(U).   RECOMMENDATIONS

        Precursor wave phenomenon should be given consideration in
the design of low sound signature weapons.

        More basic experimental data should be generated in support of
findings in this report.

        Various constitutents of silenced and unsilenced weapons sound
signatures should be analyzed individually.

        Weapon sound signatures should be interpreted in view of human
response to sound frequency, sound pressure level (SPL), duration and
intermittence.

REFERENCES

1. Greveris, H., "Gun Silencers". (Report to be published) (C) (1967), Frankford Arsenal, U. S. Army, Philadelphia, Pa.

2. Skochko, L. W., "Sound Analysis of Ballistic Shock Waves", Report No. R-1798 (1966), Frankford Arsenal, U. S. Army, Philadelphia, Pa.

3. Liepmann & Roshko, "Elements of Gasdynamics". (1957) Wiley & Sons, New York.

4. Lukasiewics, "Shock Tube Theory and Applications". (1952) AD-96, 447.

5. Corner, "Theory of the Internal Ballistics of Guns". (1950) Wiley & Sons, New York.

6. Rudinger, "Wave Diagrams for Nonsteady Flow in Ducts". (1955) D. Van Nostrand, Inc.

7. Kinsler & Frey, "Fundamentals of Acoustics". (1962) Wiley & Sons, New York.

8. Morse, P. M., "Vibration and Sound". (1948) McGraw-Hill Book Co., Inc., 312.

9. Bannister, F. K., "Wave Action Following Sudden Release of Compressed Gas from a Cylinder". Inst. Mech. Engrs. Proc. Vol. 159, War Emergency Issue No. 42. (1948)

10. Bertrand & Mathews, "Overpressures and Durations of Shock Waves Emerging from Open-Ended Shock Tubes". Ballistic Research Laboratories, Aberdeen, Md. Report No. MR-1724 (AD-633 161)

11. Garinther, G., & Moreland, J., "Transducer Techniques for Measuring the Effect of Small-Arms Noise on Hearing". Human Engineering Laboratory, Aberdeen, Md. Report No. TM 11-65. (July 1965)

REFERENCES   (Cont'd)

12.   Mayer & Hart, "Simplified Equations of Interior Ballistics".
      (1945)   Jour. Franklin Inst., 240, 401.

13.   Lighthill, F. R. S., "On Sound Generated Aerodynamically", I.
      General Theory (Proc. Roy. Soc. A, 211, 564 (1952), II. Turbu-
      lence as a Source of Sound (Proc. Roy. Soc. A, 222, 1 (1954).

57

DOCUMENT CONTROL DATA - R & D

(Security classification of title, body of abstract and indexing annotation must be entered when the overall report is classified)

1. ORIGINATING ACTIVITY (Corporate author)	2a. REPORT SECURITY CLASSIFICATION
FRANKFORD ARSENAL Philadelphia, Pa.	2b. GROUP III

3. REPORT TITLE

A SOURCE OF SMALL ARM MUZZLE NOISE (U)

4. DESCRIPTIVE NOTES (Type of report and inclusive dates)

Research Report

5. AUTHOR(S) (First name, middle initial, last name)

Leonard W. Skochko
Harry A. Greveris

6. REPORT DATE	7a. TOTAL NO. OF PAGES	7b. NO. OF REFS
August 1967	60	13

8a. CONTRACT OR GRANT NO. AMCMS Code 5542.12.46801.01 b. PROJECT NO. DA Project M1-5-16495-06-F6-NH c. d.	9a. ORIGINATOR'S REPORT NUMBER(S) R1860 9b. OTHER REPORT NO(S) (Any other numbers that may be assigned this report)

10. DISTRIBUTION STATEMENT In addition to security requirements which apply to this document and which must be met, this document is subject to special export controls and each transmittal to foreign governments or foreign nationals may be made only with prior approval of Commanding Officer, Frankford Arsenal, Phila., Pa. 19137, Attn: SMUFA-J8100.

11. SUPPLEMENTARY NOTES	12. SPONSORING MILITARY ACTIVITY U.S. Army Weapons Command Rock Island Illinois and U.S. Army Munitions Command Dover, N. J.

13. ABSTRACT

(U) This report describes and analyzes the pressure wave generated in front of small caliber subsonic projectiles traveling in gun barrel.

(U) Equations are developed to predict the precursor wave sound signature in the far field.

(U) Calculations and measured sound data are presented for several representative, conventional and unconventional, small arm weapons.

DD FORM 1473 REPLACES DD FORM 1473, 1 JAN 64, WHICH IS OBSOLETE FOR ARMY USE.

Unclassified
Security Classification

14. KEY WORDS	LINK A		LINK B		LINK C	
	ROLE	WT	ROLE	WT	ROLE	WT
Noise attenuation						
Silent weapons						
Subsonic projectiles						
Gas flow						
Precursor pressure waves						
Sound signature						
Far field sounds						